iScience

CellPress
OPEN ACCESS

Article

Receptor-specific Ca^{2+} oscillation patterns mediated by differential regulation of P2Y purinergic receptors in rat hepatocytes

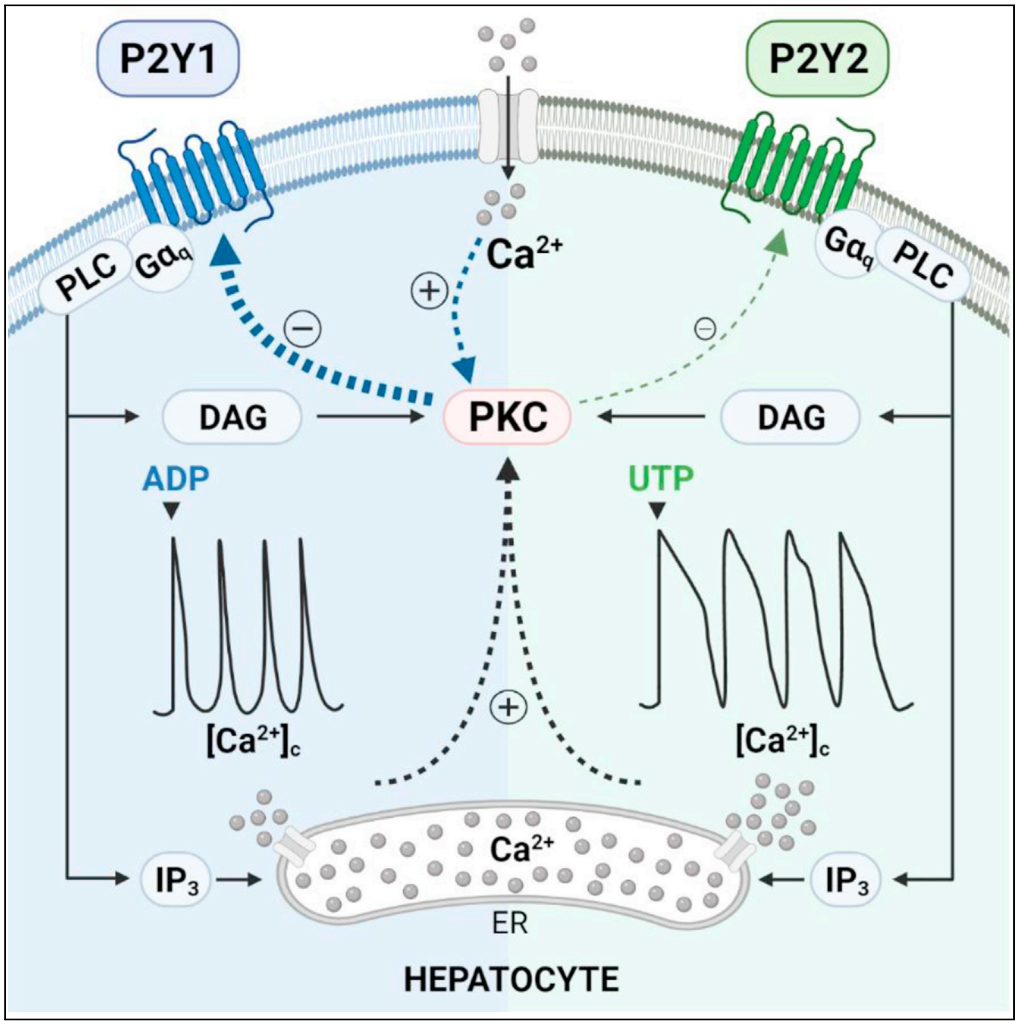

Juliana C. Corrêa-Velloso, Paula J. Bartlett, Robert Brumer, Lawrence D. Gaspers, Henning Ulrich, Andrew P. Thomas

andrew.thomas@rutgers.edu

Highlights

Distinct stereotypic Ca^{2+} oscillations are elicited by P2Y1 and P2Y2 receptors

P2X receptors do not contribute to the generation of Ca^{2+} oscillations

Agonist-specific Ca^{2+} spike shapes reflect discrete modes of PKC negative feedback

Bifurcation of IP_3/PKC signaling yields unique Ca^{2+} oscillation signatures

Corrêa-Velloso et al., iScience *24*, 103139
October 22, 2021
https://doi.org/10.1016/j.isci.2021.103139

iScience

CellPress
OPEN ACCESS

Article

Receptor-specific Ca^{2+} oscillation patterns mediated by differential regulation of P2Y purinergic receptors in rat hepatocytes

Juliana C. Corrêa-Velloso,[1] Paula J. Bartlett,[1] Robert Brumer,[1] Lawrence D. Gaspers,[1] Henning Ulrich,[2] and Andrew P. Thomas[1,3,*]

SUMMARY

Extracellular agonists linked to inositol-1,4,5-trisphosphate (IP_3) formation elicit cytosolic Ca^{2+} oscillations in many cell types, but despite a common signaling pathway, distinct agonist-specific Ca^{2+} spike patterns are observed. Using qPCR, we show that rat hepatocytes express multiple purinergic P2Y and P2X receptors (R). ADP acting through P2Y1R elicits narrow Ca^{2+} oscillations, whereas UTP acting through P2Y2R elicits broad Ca^{2+} oscillations, with composite patterns observed for ATP. P2XRs do not play a role at physiological agonist levels. The discrete Ca^{2+} signatures reflect differential effects of protein kinase C (PKC), which selectively modifies the falling phase of the Ca^{2+} spikes. Negative feedback by PKC limits the duration of P2Y1R-induced Ca^{2+} spikes in a manner that requires extracellular Ca^{2+}. By contrast, P2Y2R is resistant to PKC negative feedback. Thus, the PKC leg of the bifurcated IP_3 signaling pathway shapes unique Ca^{2+} oscillation patterns that allows for distinct cellular responses to different agonists.

INTRODUCTION

Cytosolic Ca^{2+} ($[Ca^{2+}]_c$) oscillations are key regulators of cellular signaling and tissue physiology in a variety of cell types (Berridge et al., 2003; Clapham, 2007). In hepatocytes, oscillatory $[Ca^{2+}]_c$ transients play a key role in bile secretion (Schlosser et al., 1996), regulation of mitochondrial oxidative phosphorylation (Hajnoczky et al., 1995), glucose metabolism (Exton, 1987; Gaspers et al., 2019), and tissue regeneration and gene expression (Lagoudakis et al., 2010). Hepatocytes comprise about 80% of the liver volume, but Ca^{2+} signaling is also important in other liver cell types, including biliary epithelial cells (cholangiocytes), stellate cells, Kupffer cells (hepatic macrophages) and liver sinusoidal endothelial cells (Trefts et al., 2017). In both isolated hepatocytes and hepatocytes of the intact liver, oscillatory increases in $[Ca^{2+}]_c$ elicited by hormones such as vasopressin and the catecholamines epinephrine and norepinephrine are well described (Woods et al., 1986; Rooney et al., 1989; Sanchez-Bueno and Cobbold, 1993; Robb-Gaspers and Thomas, 1995; Gaspers and Thomas, 2005). These agonists act through $G\alpha_q$-linked G-protein-coupled receptors (GPCRs) to activate phosphoinositide-specific phospholipase C (PLC), resulting in the hydrolysis of phosphatidylinositol 4,5-bisphosphate (PIP_2) into inositol 1,4,5-triphosphate (IP_3) and diacylglycerol (DAG). IP_3 mobilizes Ca^{2+} from the ER via IP_3 receptors (IP_3R), and DAG recruits and activates protein kinase C (PKC) to initiate specific protein phosphorylation cascades (Patel et al., 1999; Zeng et al., 2012). PKC isoforms can be divided into three subfamilies based on their primary structure and biochemical characteristics. Classical or conventional PKC isoforms (PKCα, βI, βII and γ) are activated by phosphatidylserine, Ca^{2+}, and DAG or phorbol esters, whereas novel nPKCs (PKCδ, ε, θ and η) are activated by phosphatidylserine, DAG or phorbol esters but not by Ca^{2+}. Atypical aPKCs (PKCζ, λ in mouse and ι in human) require neither Ca^{2+} nor DAG for activation (Steinberg, 2008). Modulation of PKC, by activation or inhibition of its isoforms, can modify hormone-induced $[Ca^{2+}]_c$ oscillation frequency and duration (Bartlett et al., 2015; Berrie and Cobbold, 1995; Sanchez-Bueno et al., 1990).

In hepatocytes, Ca^{2+} spike frequency is controlled by the agonist concentration, which encodes stimulus strength and determines the magnitude of downstream responses, whereas Ca^{2+} spike amplitude and kinetics are independent of the agonist dose (Woods et al., 1986; Rooney et al., 1989; Thomas et al., 1991; Gaspers and Thomas, 2005; Bartlett et al., 2014). The $[Ca^{2+}]_c$ oscillation rising phase is driven by positive feedback of Ca^{2+} on the IP_3R and PLC-β (Bartlett et al., 2020; Gaspers et al., 2014; Politi et al., 2006) and

[1]Department of Pharmacology, Physiology & Neuroscience, New Jersey Medical School, Rutgers, The State University of New Jersey, Newark, NJ 07103, USA

[2]Department of Biochemistry, Institute of Chemistry, University of São Paulo, São Paulo, Brazil

[3]Lead contact

*Correspondence: andrew.thomas@rutgers.edu

https://doi.org/10.1016/j.isci.2021.103139

is also relatively constant irrespective of the GPCR activated. However, there is agonist-specific diversity in the falling phase of the Ca^{2+} spikes, which gives rise to receptor-specific spike profiles that are remarkably distinguishable for each individual biological trigger (Dixon et al., 1990; Gaspers et al., 2014; Rooney et al., 1989). This Ca^{2+} spike decay phase sets the duration of the $[Ca^{2+}]_c$ transient, an important parameter that has been demonstrated to regulate activation of gene-specific transcription factors (Vilborg et al., 2016). Therefore, elucidation of the signaling machinery that regulates Ca^{2+} spike kinetics in an agonist-specific manner is key to understanding how physiological information is encoded by $[Ca^{2+}]_c$ oscillations.

Extracellular nucleotides are key signaling molecules, recognized by hepatocytes and other liver cell types, affecting important hepatic processes (Burnstock et al., 2014). ATP binds to purinergic P2 receptors, a family of cell-surface receptors which have been divided into two classes based on their structures and modes of signal transduction: ligand-gated ion channels termed P2X receptors and GPCRs termed P2Y receptors. P2X receptors are ATP-gated ion channels permeable to Na^+, K^+, and Ca^{2+} cations (Ralevic and Burnstock, 1998). Seven subunits of these receptors (P2X1-7) expressed by different cell types are grouped either in a homomeric or heteromeric mode (Barrera et al., 2005). P2Y receptors are metabotropic and activated by purines and pyrimidines, including ATP, ADP, UTP, UDP, or UDP-glucose, and they are subclassified into P2Y1, 2, 4, 6, 11, 12, 13, and 14 subtypes (Abbracchio et al., 2006) (P2Y11 receptor has been described only in humans (Kennedy, 2017)). P2Y1, 2, 4, 6, and 11 receptors are coupled to $G\alpha_q/_{11}$ G-proteins, leading to activation of the PLC - IP_3 pathway and subsequent Ca^{2+} release from ER. P2Y12, 13 and 14 subtypes are coupled to G_I and G_o, inhibiting adenylate cyclase and leading to decreased activity of cAMP-dependent protein kinase. Activation of these receptors does not result in a direct change in $[Ca^{2+}]_c$ (Erb and Weisman, 2012). Alterations in purinergic signaling mediated by distinct receptor types have been described in models of vascular injury, inflammation, insulin resistance, hepatic fibrosis, cirrhosis, diabetes, hepatitis, liver regeneration following injury or transplantation, and cancer (Vaughn et al., 2014). For example, P2Y2 receptor signaling is specifically required for hepatocyte proliferation, and knockout of the P2Y2 receptor impairs this process after partial hepatectomy (Tackett et al., 2014). However, little is known about the physiological role of extracellular nucleotides in the healthy liver, and how distinct purinergic receptors, potentially responding to different nucleotides, give rise to different downstream responses.

The first reports of the characterization of extracellular nucleotide-induced $[Ca^{2+}]_c$ oscillations in hepatocytes were performed in primary rat cells microinjected with the Ca^{2+} indicator aequorin (Dixon et al., 1990, 1993, 1995, 2000, 2003, 2004). These studies characterized the pharmacology of hepatic purinergic receptors involved in Ca^{2+} signaling and investigated downstream effects on metabolism. In the present study, we have used fura-2 Ca^{2+} imaging to study $[Ca^{2+}]_c$ oscillations, similar to those described previously (Dixon et al., 1990, 1993, 1995; Green et al., 1994; Rooney et al., 1989; Thomas et al., 1991). Submaximal doses of endogenous purinergic agonists elicited discretely distinguishable $[Ca^{2+}]_c$ spike patterns for agonists known to act on different purinergic receptor subtypes. We found that the predominant P2Y receptors in rat hepatocytes were P2Y1, which is activated by ADP and yields short duration $[Ca^{2+}]_c$ spikes, and P2Y2, which is activated by UTP to give longer duration more complex $[Ca^{2+}]_c$ spike patterns. ATP activates these two P2Y receptor subtypes and generates complex composite $[Ca^{2+}]_c$ oscillation patterns. An important question is what receptor-specific mechanisms give rise to the distinct stereotypic shape and duration of the individual $[Ca^{2+}]_c$ spikes? Previous studies have shown that rat hepatocytes also have functional P2X receptors that could contribute to the $[Ca^{2+}]_c$ oscillations in response to ATP (Gonzales et al., 2007). However, we found that the P2X receptors were not activated at the physiological doses of ATP that give rise to $[Ca^{2+}]_c$ oscillations in hepatocytes. Instead, our studies demonstrate that P2Y1 receptor activation with ADP elicits narrow $[Ca^{2+}]_c$ transients due to robust negative feedback by PKC and that this effect of PKC is largely driven by Ca^{2+} influx at the plasma membrane. By contrast, the P2Y2 receptors activated by UTP generate broad $[Ca^{2+}]_c$ transients, which are less sensitive to PKC-dependent negative regulation and independent of Ca^{2+} influx. Thus, distinct receptor-specific feedbacks by PKC underlie the unique stereotypic $[Ca^{2+}]_c$ oscillation patterns elicited by different PLC-linked GPCRs.

RESULTS

$[Ca^{2+}]_c$ oscillation characteristics and types of responses elicited by purinergic agonists

Activation of purinergic receptors has been shown to generate a diverse pattern of $[Ca^{2+}]_c$ oscillations (Dixon et al., 1990, 2000, 2004, 2005; Schofl et al., 1999), although the specific contribution of each of the P2X and P2Y receptor types has not been fully described. In order to distinguish the Ca^{2+} responses elicited by different types of purinergic receptors, $[Ca^{2+}]_c$ oscillation responses to ATP, ADP, UTP, and UDP were

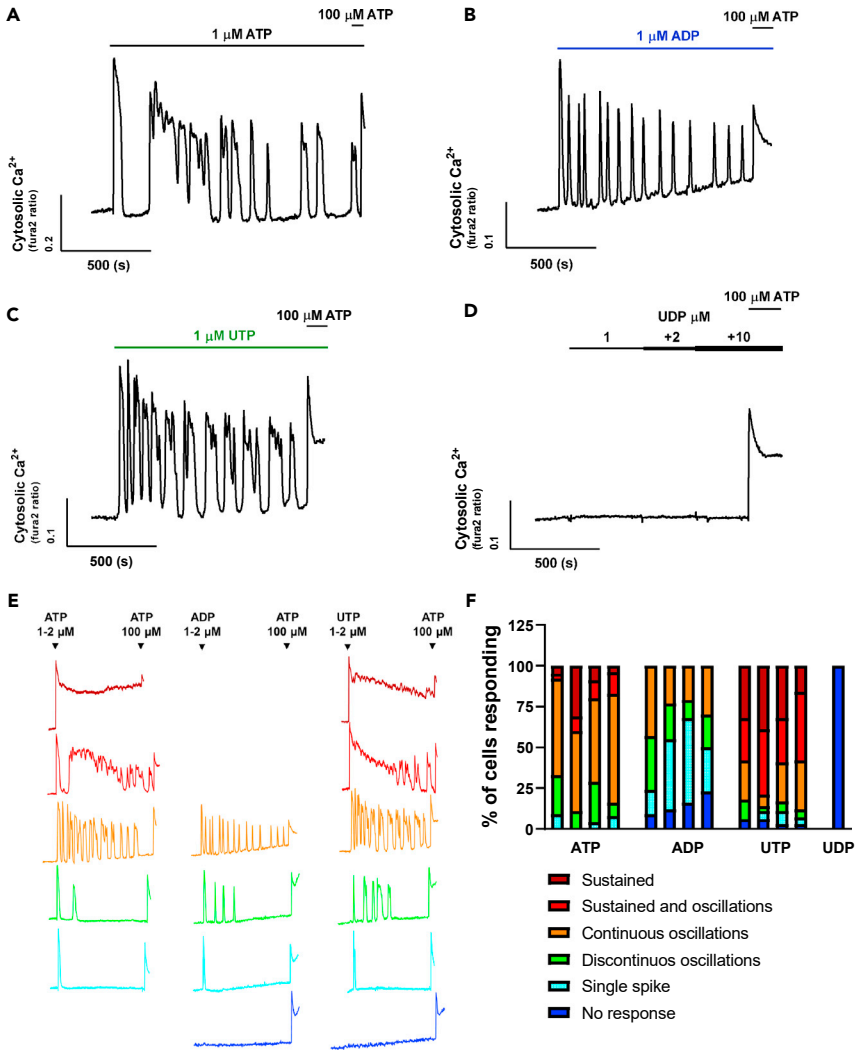

Figure 1. $[Ca^{2+}]_c$ oscillation profiles elicited by purine nucleotides in hepatocytes

(A–D) Representative traces of typical ATP (A), ADP (B), UTP (C), and UDP-induced (D) $[Ca^{2+}]_c$ responses in hepatocytes loaded with fura-2. The duration of exposure and concentration of each nucleotide is indicated in the bars above each trace.

(E) The indicated agonist was present continuously from the first addition arrow, followed by a maximal dose of ATP (100 μM) at the second arrow. At low agonist doses (1–2 μM), different strengths of Ca^{2+} response from *No response* (blue), *Single spike* (cyan), *Discontinuous oscillations* (green), *Continuous Oscillations* (orange), *Sustained & oscillations* (red) through to *Sustained* (dark red) can be elicited by each extracellular nucleotide.

(F) Ordinal plot of the Ca^{2+} response strength in hepatocytes challenged with ATP, ADP, UTP, or UDP. (Data are from ≥50 cells in each of four independent experiments).

analyzed in freshly isolated rat hepatocytes. At low physiological doses (1–5 μM), the spike kinetics of $[Ca^{2+}]_c$ oscillations were different, with distinguishable falling phases, indicating that the duration of the individual Ca^{2+} spikes is characteristic of the purinergic receptor being activated (Figure 1). Similar receptor-specific Ca^{2+} spike shapes have been reported for other $G_{\alpha q}$-coupled receptors, including V_1-vasopressin and α_1-adrenergic receptors (Rooney et al., 1989; Bartlett et al., 2014; Sanchez-Bueno and Cobbold, 1993).

ATP, an agonist for all ionotropic P2X and metabotropic P2Y receptors, elicited complex $[Ca^{2+}]_c$ oscillations with two main patterns: broad Ca^{2+} spikes with small secondary oscillations resulting in a biphasic decay phase, and narrow Ca^{2+} spikes with a fast decay phase. Although both patterns can be observed in the same cell, broad Ca^{2+} spikes of relatively long duration were observed in the majority of

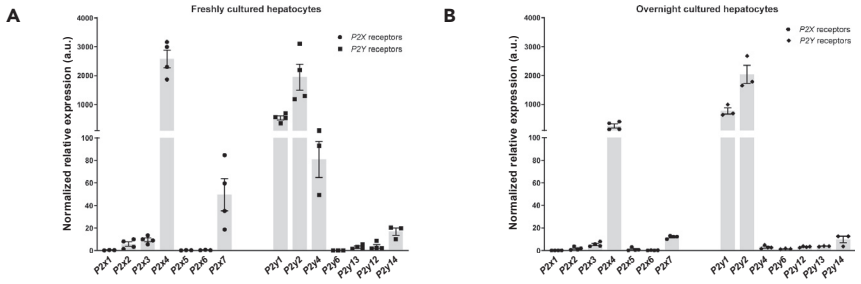

Figure 2. Purinergic P2 receptor gene expression in primary rat hepatocytes

(A and B) RT-qPCR determination of mRNA expression levels of P2X and P2Y receptors from freshly isolated (A) and overnight (B) cultured hepatocytes. Purinergic receptor gene expression was normalized to *Rpl0* expression. Data are mean ± S.E.M from 3 to 4 hepatocyte preparations in each case. See Table S1 for primer details.

ATP-stimulated hepatocytes (Figure 1A). Spike width (measured as full width at half maximum; FWHM) of baseline-separated ATP-evoked $[Ca^{2+}]_c$ oscillations were 35.6 ± 3.5 s for the more complex broad Ca^{2+} spikes and 18.6 ± 2.1 s for the short duration Ca^{2+} spikes. ADP, an agonist of $G\alpha_q$-coupled P2Y1 and G_i-coupled P2Y12 and P2Y13 receptors, generated homogeneous short duration $[Ca^{2+}]_c$ oscillations (15.9 ± 0.9 s FWHM) with narrow peaks and a rapid declining phase, similar to the sporadic narrow Ca^{2+} spikes induced by ATP (Figure 1B). UTP, an agonist of P2Y2 and P2Y4 receptors, elicited predominantly longer duration Ca^{2+} spikes (40.4 ± 3.5 s), similar to the broad long duration ATP responses (Figure 2C). UDP, a P2Y6 receptor-selective nucleotide, was the only purinergic agonist tested that failed to elicit a $[Ca^{2+}]_c$ response in rat hepatocytes (Figure 1D).

As noted in the Introduction, the signal strength for Ca^{2+}-dependent hormones such as vasopressin and norepinephrine in hepatocytes is not a function of $[Ca^{2+}]_c$ oscillation amplitude, which is relatively constant, but is encoded in the frequency, duration and robustness (maintenance) of the $[Ca^{2+}]_c$ oscillations (Rooney et al., 1989; Woods et al., 1986; Gaspers et al., 2014). These $[Ca^{2+}]_c$ responses can be classified using an ordinal scale ranging from no response, through single spikes, then oscillations and up to a sustained $[Ca^{2+}]_c$ increase. Stimulation of different receptors by each extracellular nucleotide evoked not only distinct Ca^{2+} spike profiles but also a different range in the magnitude of $[Ca^{2+}]_c$ response (Figures 1E and 1F). ATP was able to elicit all types of $[Ca^{2+}]_c$ responses, from single spikes to a fully sustained increase (Figure 1E, left panel) and was the only nucleotide able to evoke an increase in $[Ca^{2+}]_c$ in all analyzed cells (Figure 1F). P2Y2/P2Y4 receptor activation by UTP generated mostly large initial $[Ca^{2+}]_c$ peaks followed by a sustained plateau and repetitive broad Ca^{2+} spikes (Figures 1E, right panel and 1F). Activation of P2Y1 receptors by ADP evoked only a range of single, irregular or repetitive narrow $[Ca^{2+}]_c$ oscillations without any sustained $[Ca^{2+}]_c$ signals (Figures 1E, middle panel and 1F).

mRNA expression of P2 receptors in primary rat hepatocytes

cDNAs generated from five independent rat hepatocyte preparations were probed by RTqPCR using primers specific for P2X and P2Y receptors (Figure 2). Low mRNA expression levels of P2X receptors *P2x1*, *P2x2*, *P2x3*, *P2x5,* and *P2x6* were detected, whereas *P2x4* and *P2x7* transcripts were abundantly expressed in both freshly isolated and overnight-cultured hepatocytes. For the $G_{\alpha q}$-coupled P2Y receptors, *P2y1*, *P2y2,* and *P2y4* subtypes were abundantly observed, with very low transcript detection of *P2y6*. After overnight culture, a considerable decrease in *P2y4* expression was observed (Figure 2B), resulting in expression of predominantly *P2y1* and *P2y2* $G_{\alpha q}$-coupled receptors. The G_i-coupled *P2y12*, *P2y13,* and *P2y14* receptors were detected, albeit at a low expression levels at both time points analyzed. Thus, according to the expression profile, mRNA transcripts mainly from *P2x4*, *P2x7*, *P2y1*, *P2y2,* and *P2y4* were detected in rat hepatocytes, consistent with relevant physiological roles for these receptors.

P2X receptors do not contribute to $[Ca^{2+}]_c$ oscillations in rat hepatocytes

The similarity of the oscillatory $[Ca^{2+}]_c$ responses induced by ATP and UTP to those elicited by other $G\alpha_q$-coupled receptors (Rooney et al., 1989; Woods et al., 1986) suggests that these purinergic Ca^{2+} signals arise predominantly from IP_3-dependent mobilization of intracellular Ca^{2+} stores through activation of P2Y receptors. However, since abundant mRNA expression of the P2X4 and P2X7 receptors was observed, we designed experiments to determine whether P2X receptors contribute to the observed $[Ca^{2+}]_c$ signals.

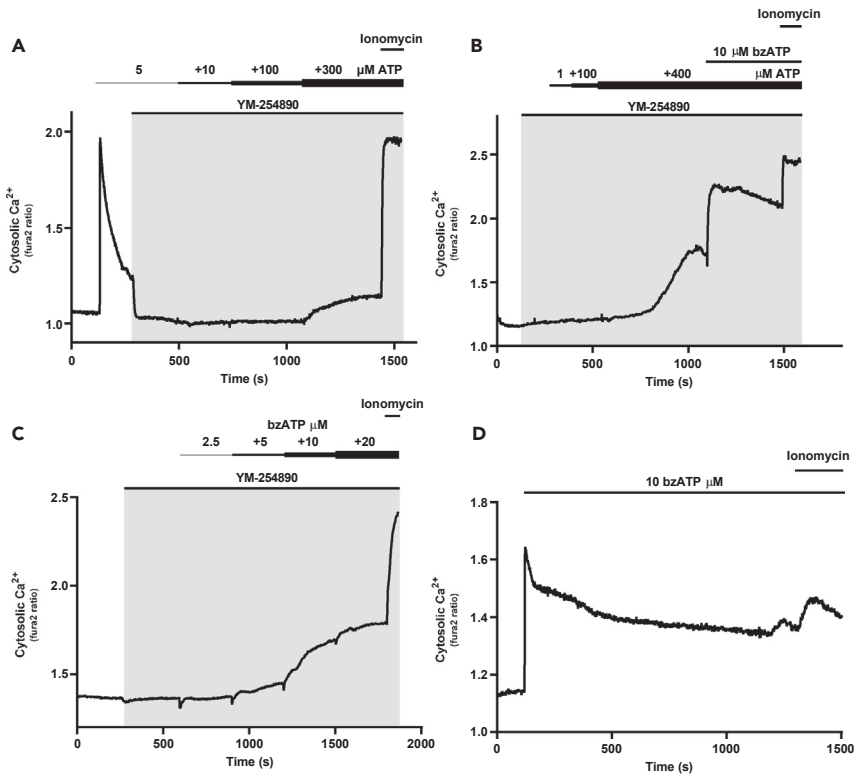

Figure 3. P2X receptor activity does not contribute to $[Ca^{2+}]_c$ oscillations in hepatocytes

Hepatocytes loaded with fura-2 were exposed to the indicated concentrations of ATP (in μM). The $G\alpha_q$ protein inhibitor YM-254890 (1 μM) was present during the period indicated by the gray shading.

(A) ATP (5 μM) induced a large $[Ca^{2+}]_c$ spike that was terminated by addition of YM-254890. Subsequent additions of increasing concentrations of ATP (10 and 100 μM) had no effect on $[Ca^{2+}]_c$, whereas a high ATP dose (300 μM) caused a slow monophasic $[Ca^{2+}]_c$ increase.

(B) Effect of increasing ATP concentrations in the presence of YM-254890, followed by addition of the P2X agonist BzATP (10 μM).

(C) Dose response to BzATP in the presence of YM-254890.

(D) Response to BzATP (10 μM) in the absence of YM-254890.

We used YM-254890, a specific inhibitor for $G\alpha_q$ (Uemura et al., 2006) to block P2Y receptor coupling to this G-protein in freshly isolated hepatocytes. Addition of 1 μM YM-254890 reversed the $[Ca^{2+}]_c$ response elicited by 5 μM ATP (Figure 3A), and blocked all $[Ca^{2+}]_c$ responses to ATP concentrations of 1–100 μM (Figures 3A and 3B). At higher ATP concentrations (300–400 μM), a slow $[Ca^{2+}]_c$ increase to a plateau level was observed (Figures 3B and 3C), suggesting that P2X receptor activation and Ca^{2+} influx through the associated plasma membrane channels only occurs at very high ATP concentrations. ATP never elicited $[Ca^{2+}]_c$ oscillations in the presence of YM-254890. Consistent with a role for P2X receptors at high ATP concentrations, the P2X4/P2X7 receptor agonist BzATP (10–20 μM) also caused a monophasic $[Ca^{2+}]_c$ increase in the presence of YM-254890 (Figures 3B and 3C), and similar to ATP, BzATP did not cause $[Ca^{2+}]_c$ oscillations under these conditions. Even when added in the absence of YM-254890, 10 μM BzATP caused a sustained $[Ca^{2+}]_c$ increase without oscillations (Figure 3D). At lower concentrations of BzATP, $[Ca^{2+}]_c$ oscillations were sometimes observed in the absence of YM-254890, consistent with the partial agonist activity of BzATP against P2Y1 receptors (Gonzales et al., 2007; Ohtomo et al., 2011).

P2Y1 and P2Y2 receptors evoke distinct stereotypic $[Ca^{2+}]_c$ spike patterns in rat hepatocytes

Based on the data described above, it appears that activation of specific P2Y purinergic receptors subtypes determines the kinetics of the periodic Ca^{2+} transients (primarily in the Ca^{2+} spike falling phase), and hence gives rise to the distinct $[Ca^{2+}]_c$ oscillation pattern generated by different agonists. Rat P2Y2 and P2Y4 receptors can be activated equipotently by ATP and UTP (Bogdanov et al., 1998; Webb et al., 1998), and P2Y1, P2Y12, and P2Y13 can be activated by ADP (Abbracchio et al., 2006). The absence of any response to ATP in

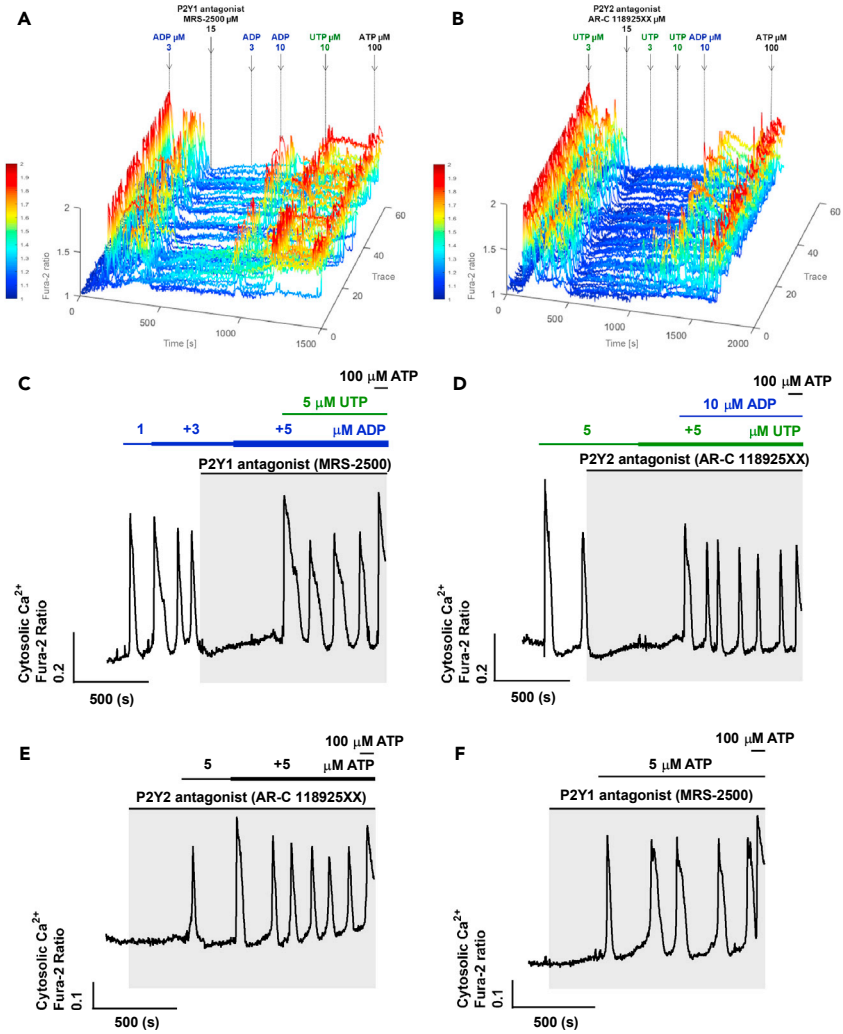

Figure 4. Role of P2Y1 and P2Y2 purinergic receptors

(A and B) Normalized and color-mapped view of traces from 60 rat hepatocytes loaded with fura-2. Cells were challenged as indicated with 15 μM MRS-2500, an antagonist of P2Y1 receptor (A), and 15 μM AR-C 118925XX, an antagonist of P2Y2 receptor (B). The indicated concentration of each nucleotide was added at the arrows and remained present for the remainder of the experiment. A maximal dose of ATP (100 μM) was added at the end of the experiment.

(C and D) Representative traces of treatment with MRS-2500 and AR-C 118925XX, as indicated by the shaded areas, and treatment with ADP and UTP (C) or UTP and ADP (D).

(E and F) Representative traces for pretreatment with MRS-2500 (E) and AR-C 118925XX (F) followed by ATP stimulation.

the presence of YM-254890 (Figure 3), suggests that the relatively low expressed G_i-coupled P2Y12, P2Y13, and P2Y14 receptor subtypes do not underlie the $[Ca^{2+}]_c$ oscillations. This leaves P2Y1, P2Y2, and P2Y4 receptors. P2Y1 and P2Y2 receptors have previously been described as active in hepatocytes and shown to be sensitive to the nonspecific antagonists suramin and pyridoxal phosphate-6-azo(benzene-2,4-disulfonic acid) (PPADS) (Dixon et al., 2000; Thevananther et al., 2004). To distinguish the receptors activated by ADP and UTP in rat hepatocytes, we used antagonists specifically targeted to P2Y1 and P2Y2 receptors, respectively.

The effects of MRS-2500, a selective antagonist for P2Y1 receptor, and AR-C 118925XX, a selective and competitive antagonist for P2Y2 receptor, are shown in Figures 4A and 4B, respectively. Ca^{2+} imaging traces from 60 hepatocytes in a single imaging field were normalized and plotted side by side in 3-D space with a color gradient. Narrow ADP-induced $[Ca^{2+}]_c$ oscillations were blocked by MRS-2500

(Figures 4A and 4C). In the continuing presence of MRS-2500, further additions of ADP (3-5 μM) did not induce a resumption of the $[Ca^{2+}]_c$ oscillations, although higher ADP doses (10 μM) elicited a weak Ca^{2+} increase in some cells. Consistent with the known agonist sensitivity of the P2Y1 receptor, these data demonstrate that the narrow $[Ca^{2+}]_c$ oscillations induced by ADP in rat hepatocytes are driven by P2Y1 receptors. After P2Y1 inhibition, subsequent stimulation with UTP generated a robust $[Ca^{2+}]_c$ response (Figure 4A), with broad Ca^{2+} spikes (Figure 4C). In separate experiments, UTP receptor specificity was assessed with AR-C 118925XX, which completely blocked the broad UTP-induced $[Ca^{2+}]_c$ oscillations (Figures 4B and 4D). Stepping up the concentration of UTP (3–10 μM) in the continuing presence of AR-C 118925XX, did not elicit a $[Ca^{2+}]_c$ increase (Figures 4B and 4D). The absence of a $[Ca^{2+}]_c$ response to UTP after P2Y2 receptor blockage indicates that this nucleotide acts specifically through P2Y2 receptors, and P2Y4 receptors are not involved in the generation of $[Ca^{2+}]_c$ oscillations in rat hepatocytes. Importantly, in the presence of AR-C 118925XX, subsequent stimulation of P2Y1 receptors with ADP evoked the typical narrow $[Ca^{2+}]_c$ oscillations (Figure 4D).

In support of the concept that the complex $[Ca^{2+}]_c$ oscillations elicited by ATP represent a composite response to P2Y1 and P2Y2 receptor activation, the $[Ca^{2+}]_c$ oscillations elicited by ATP in the presence of the selective antagonists took on the unique characteristics of the unblocked receptor. Thus, blockage of P2Y1 receptors with MRS-2500 followed by ATP stimulation led to broad $[Ca^{2+}]_c$ oscillations (spike FWHM of 41.5 ± 5.3 s), consistent with the response to UTP mediated by P2Y2 receptors (Figure 4E). By contrast, ATP stimulation after blockage of P2Y2 receptors with AR-C 118925XX resulted in narrow $[Ca^{2+}]_c$ oscillations (spike FWHM of 22.3 ± 2.8 s) (Figure 4F).

To exclude the possibility that the differences in $[Ca^{2+}]_c$ oscillation patterns seen with ADP and UTP might reflect the generation of other components by ectonucleotidases, we evaluated the $[Ca^{2+}]_c$ responses evoked by both agonists in the presence of ARL 67156, an inhibitor of nucleoside triphosphate diphosphohydrolase-1 (CD39) and ecto-5′-nucleotidase (CD73) (Schakel et al., 2020). Preincubation for 5 min with ARL 67156 (100 μM), did not change the spike with of the typical narrow ADP-induced $[Ca^{2+}]_c$ oscillations (22.8 ± 1.3 s vs 21.3 ± 1.0 s; ADP and ARL 67156 + ADP, respectively). Similarly, the broad UTP-induced $[Ca^{2+}]_c$ oscillations were unaffected by the ectonucleotidase inhibitor (48.3 ± 1.6 s vs 45.8 ± 1.5 s; UTP and ARL 67156 + UTP, respectively) (Figure S1). Taken together, these data demonstrate that activation of P2Y1 receptor by ADP and P2Y2 receptor by UTP generate distinct stereotypic $[Ca^{2+}]_c$ oscillation patterns in rat hepatocytes.

Downregulation of PKC increases the Ca^{2+} spike width and reduces $[Ca^{2+}]_c$ oscillation frequency for purinergic agonists

The $[Ca^{2+}]_c$ oscillations elicited by activation of P2Y1 and P2Y2 receptors have characteristically distinct Ca^{2+} spike shapes that are likely to result in diverse physiological roles in the liver. The molecular mechanisms that contribute to distinct P2Y receptor-induced $[Ca^{2+}]_c$ oscillation patterns remain to be resolved. It has been shown previously that PKC activation or inhibition can have multiple effects on hormone-induced Ca^{2+} oscillation kinetics and frequency in hepatocytes (Bartlett et al., 2015; Berrie and Cobbold, 1995; Sanchez-Bueno et al., 1990). We examined the effect of downregulation of conventional and novel PKC isoforms by overnight treatment (16–24 h) with 1 μM phorbol 12-myristate 13-acetate (PMA), referred to as PKC-DR cells, or the inactive analog 4α-PMA, referred to as CTR cells. In these overnight cultured hepatocytes, the distinctive $[Ca^{2+}]_c$ oscillation patterns for ADP and UTP were still observed in the CTR cells (Figures 5A vs 5F). In both ADP- and UTP-stimulated PKC-DR cells, the $[Ca^{2+}]_c$ oscillation frequency was reduced and the spike width (FWHM) was prolonged when compared with the control cells (Figure 5). Although PKC-DR showed similar effects for both purinergic receptor agonists, the magnitude of the effect was not the same. PKC-DR cells stimulated with ADP showed a 1.8-fold increase in Ca^{2+} spike duration (17.5 ± 0.5 s to 31.1 ± 0.9 s; CTR and PKC-DR, respectively; $p < 0.0001$) (Figure 5C), whereas UTP stimulation of PKC-DR cells resulted in a more modest 1.3-fold increase in Ca^{2+} spike width (27.7 ± 0.5 s to 35.5 ± 0.7 s; CTR and PKC-DR, respectively; $p < 0.001$) (Figure 5H). Notably, the basal Ca^{2+} spike width for ADP in control (CTR) cells is about 10 s shorter than for UTP ($p < 0.0001$), but the spike widths and overall $[Ca^{2+}]_c$ oscillation shapes became more similar after PKC-DR (Figure 5). PKC-DR also had a differential effect on the magnitude of the $[Ca^{2+}]_c$ response elicited by P2Y1 and P2Y2 receptors in hepatocytes. Specifically, PKC-DR resulted in a more robust ADP response profile, with a shift to fewer unresponsive cells and an increase in oscillatory and sustained $[Ca^{2+}]_c$ responses (Figure 5E). By contrast, there was no shift in the pattern

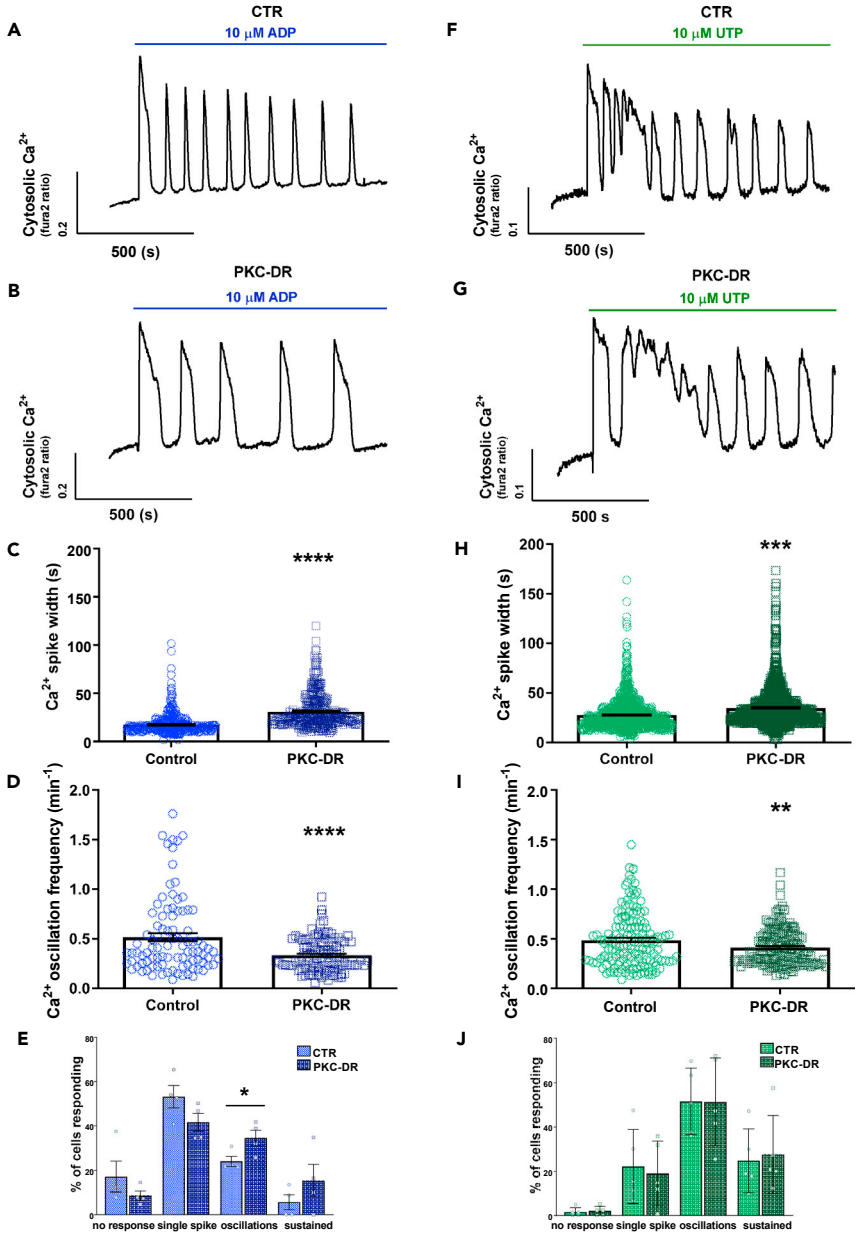

Figure 5. Downregulation of PKC prolongs ADP- and UTP-induced Ca^{2+} spike duration in isolated rat hepatocytes

Isolated hepatocytes were cultured overnight with PMA (1 μM) to downregulate conventional and novel PKC isoforms (***PKC-DR***), or with the inactive analog α-PMA (1 μM, ***CTR***). The cells were loaded with fura-2 and then stimulated with ADP or UTP as indicated.

(A, B, F and G) Representative traces for ADP- and UTP-induced $[Ca^{2+}]_c$ oscillations are shown for control (A and F) and PKC-DR hepatocytes (B and G).

(C, D, H and I) Summary data show the effects of PKC-DR on Ca^{2+} spike width measured as full width at half maximum (FWHM) and oscillation frequency for ADP- (C and D) and UTP- (H and I) induced $[Ca^{2+}]_c$ oscillations.

(E and J) The distribution of Ca^{2+} response patterns are also shown for ADP (E) and UTP (J). Blue and green symbols represent data from ADP- and UTP-induced $[Ca^{2+}]_c$ responses, respectively. Data are mean ± S.E.M. from ≥50 cells from at least three independent experiments. *, $p < 0.05$; **, $p < 0.01$; ***, $p < 0.001$; ****$p < 0.0001$; Student's t test.

of $[Ca^{2+}]_c$ response signatures in PKC-DR cells after UTP challenge (Figure 5J). The differential susceptibility of P2Y receptor-dependent $[Ca^{2+}]_c$ oscillations to PKC downregulation suggests that P2Y1 receptors are more sensitive to negative feedback inhibition by PKC than P2Y2 receptors (see Discussion).

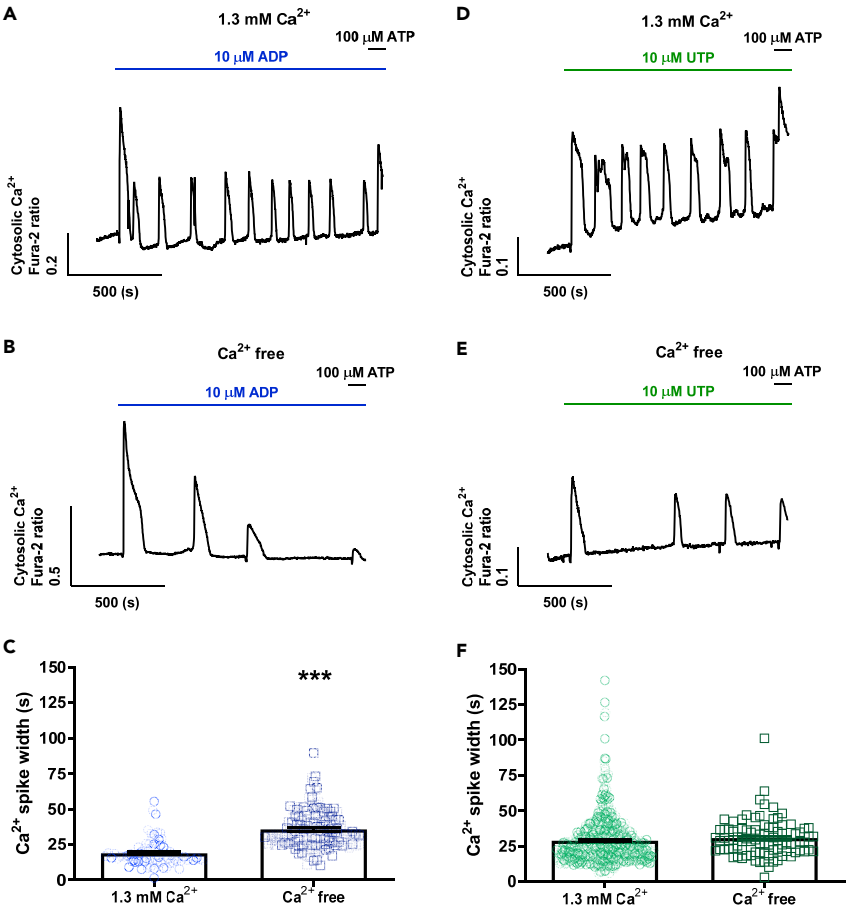

Figure 6. Absence of extracellular Ca^{2+} differentially affects P2Y1 and P2Y2 receptor-dependent $[Ca^{2+}]_c$ oscillations

Isolated hepatocytes cultured overnight were loaded with fura-2 and then stimulated with ADP and UTP (1–10 μM) in the presence (***1.3 mM Ca^{2+}***) or absence (***Ca^{2+} free***) of extracellular Ca^{2+}.

(A, B, D and E) Representative traces of typical ADP- (A and B) and UTP- (D and E) evoked $[Ca^{2+}]_c$ oscillations are shown.

(C and F) Summary data of the effect of extracellular Ca^{2+} removal on Ca^{2+} spike width (FWHM) for ADP (C) and UTP (F). Blue and green symbols represent data from ADP- and UTP-induced Ca^{2+} spikes, respectively. Data are mean ± S.E.M. from ≥50 cells from at least three independent experiments. ***, $p < 0.001$; Student's t test.

Extracellular Ca^{2+} is required for the PKC modulation of $[Ca^{2+}]_c$ oscillations elicited by P2Y1 receptor activation

To determine the impact of plasma membrane Ca^{2+} influx on P2Y-evoked $[Ca^{2+}]_c$ oscillations, we compared Ca^{2+} spike kinetics in the presence and absence of extracellular Ca^{2+}. Purinergic agonist-induced $[Ca^{2+}]_c$ oscillations were monitored in overnight cultured hepatocytes incubated in medium containing the normal physiological 1.3 mM $CaCl_2$ or switched to Ca^{2+} free buffer just prior to data acquisition (representative traces are shown in Figures 6A, 6B, 6D, and 6E). In the absence of extracellular Ca^{2+}, the individual ADP-induced Ca^{2+} spike widths were longer (35.64 ± 1.16 s) than those observed in the presence of extracellular Ca^{2+} (18.84 ± 1.09 s) at the same agonist dose (Figures 6A–6C). In UTP-stimulated cells, no difference was observed in Ca^{2+} spike width in the presence (29.25 ± 0.79 s) or absence of extracellular Ca^{2+} (30.79 ± 1.41 s) (Figure 6F). Although P2Y2 receptor activation with UTP in Ca^{2+}-free conditions did not result in a change of the Ca^{2+} spike width, the shape of the falling phase was qualitatively different. The characteristic UTP-induced Ca^{2+} spikes with a biphasic decay phase containing secondary small Ca^{2+} spikes (Figure 6D) (see also Figure 1C) were not observed in the absence of extracellular Ca^{2+}, resulting in a less complex falling phase (Figure 6E).

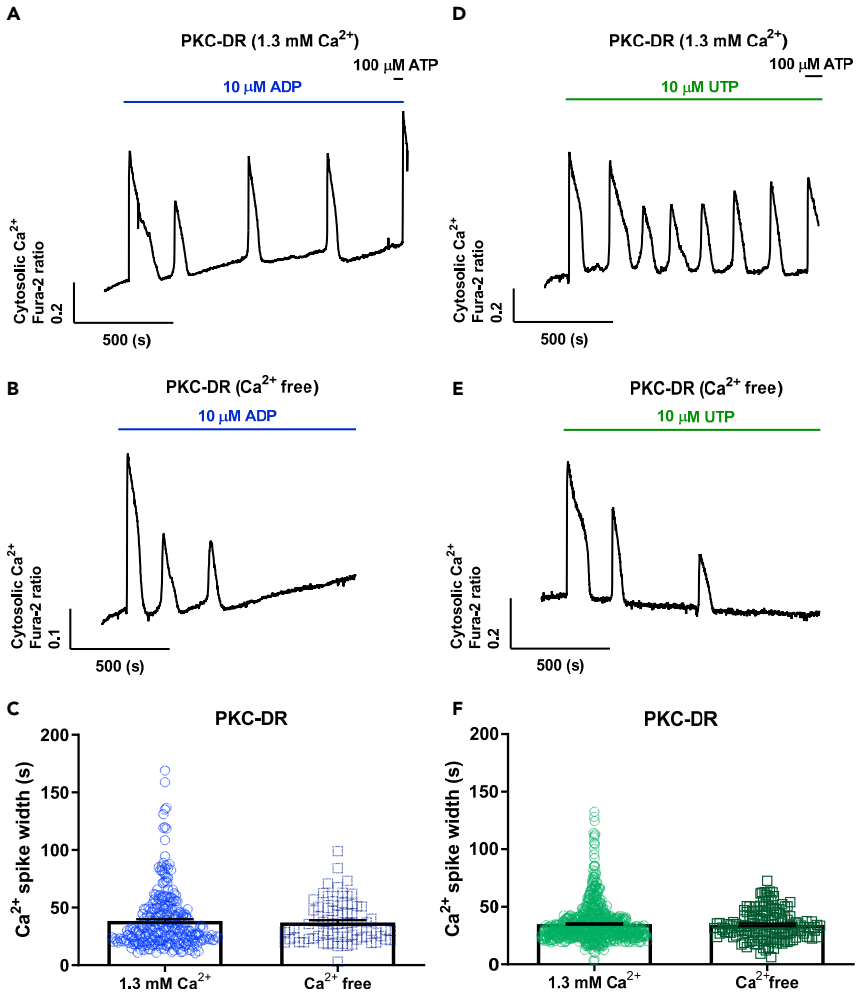

Figure 7. Extracellular Ca^{2+} has no effect on $[Ca^{2+}]_c$ oscillation spike width following PKC downregulation

Isolated hepatocytes were cultured overnight with PMA (1 μM) to downregulate conventional and novel PKC isoforms (PKC-DR).

(A, B, D and E) The cells were then loaded with fura-2 and stimulated with ADP or UTP (10–15 μM) in the presence (***1.3 mM Ca^{2+}***) or absence (***Ca^{2+} free***) of extracellular Ca^{2+}. Representative traces for ADP (A and B) and UTP (D and E) are shown under both experimental conditions.

(C and F) Summary data of the effect of extracellular Ca^{2+} removal on Ca^{2+} spike width (FWHM) in PKC-DR hepatocytes is shown for ADP (C) and UTP (F). Blue and green symbols represent data from ADP- and UTP-induced $[Ca^{2+}]_c$ oscillations, respectively. Data are mean ± S.E.M. from ≥50 cells from at least three independent experiments; Student's t test.

The data described above suggest that plasma membrane Ca^{2+} entry is required for negative feedback inhibition of P2Y1-dependent $[Ca^{2+}]_c$ oscillations elicited by ADP but not for the P2Y2-dependent $[Ca^{2+}]_c$ oscillations elicited by UTP. Thus, for P2Y1 receptors, ADP stimulation after PKC-DR or in the absence of extracellular Ca^{2+} resulted in longer duration $[Ca^{2+}]_c$ spikes, whereas P2Y2 receptor-dependent responses were affected to a lesser extent following PKC-DR and were unaffected by removal of extracellular Ca^{2+}. One possible explanation for the selective effect of extracellular Ca^{2+} on the P2Y1 responses is that plasma membrane Ca^{2+} entry could be required for negative feedback inhibition of P2Y1 receptors by PKC. To determine whether the absence of extracellular Ca^{2+} disrupts PKC-dependent regulation of Ca^{2+} spike kinetics elicited by the different P2Y receptor subtypes, we investigated whether PKC-DR affects ADP- and UTP-induced $[Ca^{2+}]_c$ responses in the presence or absence of extracellular Ca^{2+} (representative traces are shown in Figures 7A, 7B, 7D, and 7E). In PKC-DR cells, Ca^{2+} spikes elicited by P2Y1 or P2Y2 receptor activation were found to have the same duration with or without extracellular Ca^{2+} (Figures 7C and 7F). These data showing that extracellular Ca^{2+} does not affect Ca^{2+} spike width when PKC activity is

downregulated suggest that Ca^{2+} entry at the plasma membrane is important for the PKC-dependent regulation of oscillatory $[Ca^{2+}]_c$ signals.

Acute effect of PKC activation and inhibition on ADP- and UTP-induced $[Ca^{2+}]_c$ oscillations

To further investigate the role of PKC in the regulation of hepatic purinergic receptor Ca^{2+} signaling, we examined the effect of acute activation and inhibition of PKC on ADP- and UTP-induced $[Ca^{2+}]_c$ oscillations. Freshly isolated hepatocytes were stimulated with low doses of ADP or UTP (1–5 μM), to elicit $[Ca^{2+}]_c$ oscillations and then the effect of PKC modulators was determined in the same cells (representative traces are shown in Figures 8A, 8B, 8G, and 8H). $[Ca^{2+}]_c$ oscillation frequency and spike width (FWHM) were calculated in cells that displayed continuous $[Ca^{2+}]_c$ oscillations for at least 5 min before and after application of the PKC modulators. For P2Y1 receptors stimulated with ADP, activation of PKC by PMA decreased $[Ca^{2+}]_c$ oscillation frequency (Figure 8C), with no change in the spike width (Figure 8D). By contrast, for P2Y2 receptors stimulated with UTP, PKC activation with PMA did not change the $[Ca^{2+}]_c$ oscillation frequency (Figure 8I) but caused a decrease in spike width (Figure 8J). Acute inhibition of PKC with bisindolylmaleimide (BIM) had no effect on ADP- or UTP-induced $[Ca^{2+}]_c$ oscillation frequency (Figures 8E and 8L). However, BIM elicited opposite effects on the width of the Ca^{2+} spikes evoked by ADP and UTP. The spike width for ADP-induced $[Ca^{2+}]_c$ oscillations increased from 16.33 ± 1.05 s to 32.88 ± 1.55 s ($p < 0.0001$) (Figure 8F), whereas spike width for UTP-induced $[Ca^{2+}]_c$ oscillation decreased from 36.36 ± 0.65 s to 20.45 ± 0.29 s ($p < 0.0001$) (Figure 8M). A similar effect on Ca^{2+} spike duration was observed with staurosporine, a nonselective inhibitor of protein kinases, including protein kinase C (Dlugosz and Yuspa, 1991). Treatment with 500 nM staurosporine caused a small increase in the ADP-induced Ca^{2+} spike width (from 15.12 ± 0.94 s to 17.95 ± 0.77 s, $p < 0.001$), and a more pronounced decrease in Ca^{2+} spike width with UTP (from 56.24 ± 2.98 s to 22.21 ± 0.66 s, $p < 0.0001$) (Figure S2). Thus, although off-target effects of BIM and staurosporine are possible, the broadening of ADP-induced Ca^{2+} spikes and narrowing of UTP-induced Ca^{2+} spikes with both of these PKC inhibitors are consistent. Taken together, the data with acute and chronic manipulation of PKC demonstrate that this is an important feedback pathway that plays a key role in shaping the $[Ca^{2+}]_c$ oscillations elicited by purinergic agonists, and most importantly, it does so in a receptor-specific manner.

DISCUSSION

The physiological actions of extracellular nucleotides in the liver include regulation of bile secretion, glucose homeostasis and cell regeneration. At the cellular level, ATP can be released by hepatocytes into basolateral, sinusoidal, or apical extracellular compartments, acting as potent autocrine and paracrine signals to regulate liver physiology (Burnstock et al., 2014; Beldi et al., 2008). Extracellular ATP release from hepatocytes can occur through ATP permeable ion channels and via exocytosis (Fitz, 2007; Gonzales et al., 2010; Schlosser et al., 1996; Tatsushima et al., 2021). ATP accumulated into VLDL-containing vesicles in hepatocytes is co-secreted with VLDL, and this released ATP has been shown to play a role in the physiological regulation of postprandial triglycerides metabolism (Tatsushima et al., 2021). In isolated rat hepatocytes, ATP release evoked by mechanical stimulation elicits a $[Ca^{2+}]_c$ increase in the stimulated cell and also in non-adjacent neighboring cells (Schlosser et al., 1996). After hepatectomy, ATP exocytosis from hepatocytes and Kupffer cells plays an important role in liver regeneration (Gonzales et al., 2010). ATP is also released as a cotransmitter with norepinephrine from sympathetic nerves innervating the liver, and serves to stimulate glycogenolysis and gluconeogenesis through a Ca^{2+}-dependent signaling pathway (Burnstock et al., 2014). Thus, autocrine and paracrine purinergic signaling by extracellular nucleotides play multiple roles in the regulation of normal liver physiology. Moreover, under pathophysiological conditions, local release of nucleotides and/or elevated circulating levels of ATP play important roles in response to liver injury, and can also disturb the normal balance of purinergic signaling in the liver (Vaughn et al., 2012). In the present study we defined the P2X and P2Y receptors expressed in rat hepatocytes and analyzed $[Ca^{2+}]_c$ oscillations evoked by the predominant P2Y1 and P2Y2 receptors. The physiological signals encoded by these complex $[Ca^{2+}]_c$ dynamics were shown to be regulated by distinct PKC feedback mechanisms on the P2Y receptors, without any contribution of P2X receptors.

As demonstrated here and by others (Emmett et al., 2008; Gonzales et al., 2007), P2X4 and P2X7 are the most abundantly expressed P2X receptor isoforms in rat hepatocytes. Immunohistochemistry of rat liver sections showed P2X4 receptor localized in both the basolateral and apical canalicular domains of the hepatocyte (Emmett et al., 2008), consistent with the reported role of P2X4 receptors in biliary secretion (Doctor et al., 2005). Previous studies have used BzATP, an agonist of P2X4 and P2X7 receptors, to show

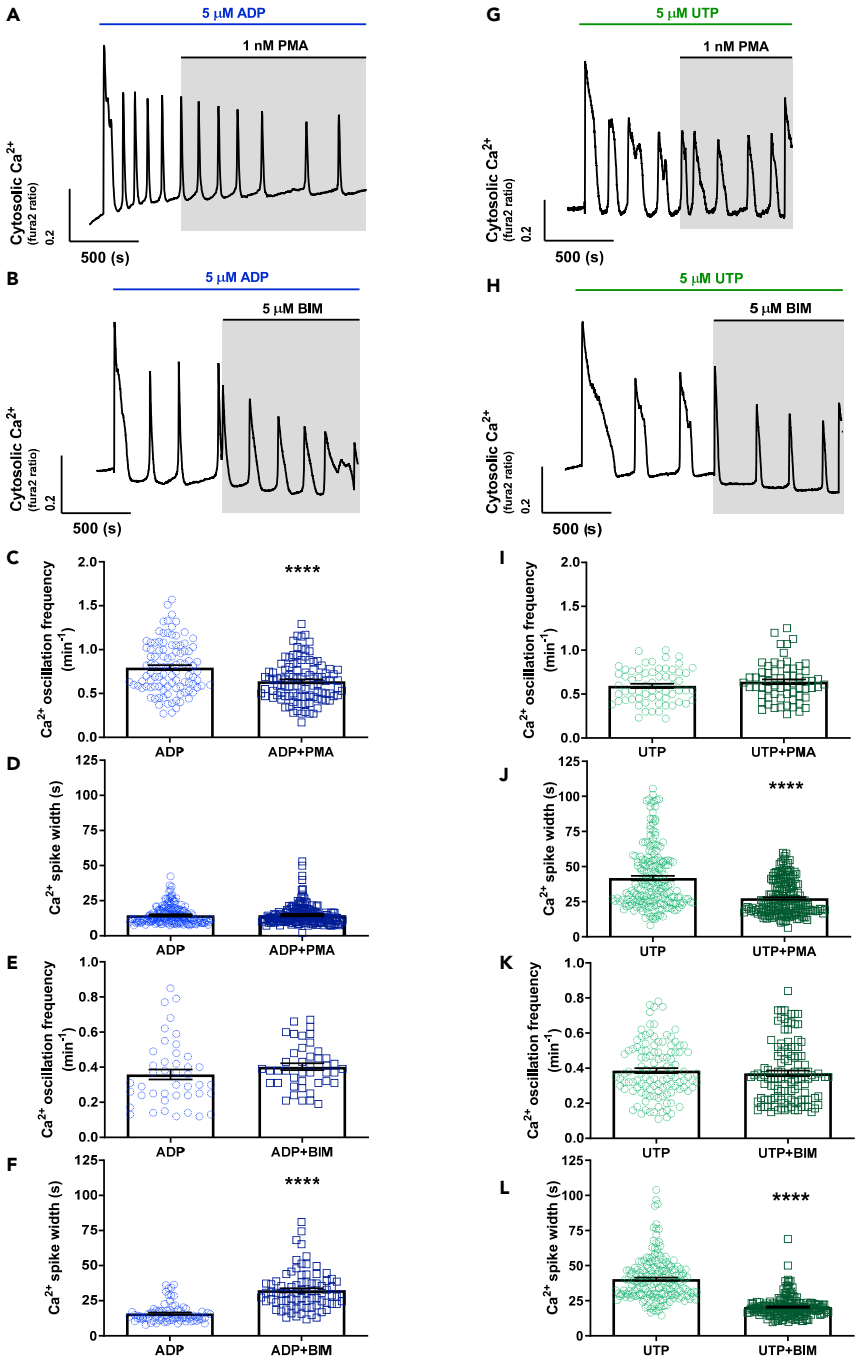

Figure 8. Effects of acute activation and inhibition of PKC on ADP- and UTP-induced $[Ca^{2+}]_c$ oscillations

The effects of PMA (1 nM) and BIM (5 μM) on ADP- and UTP-induced $[Ca^{2+}]_c$ oscillations were analyzed in rat hepatocytes loaded with fura-2. After stimulation with the purinergic agonists, cells were treated with PMA or BIM as indicated by the shaded areas on the Ca^{2+} traces.

(A, B, G, and H) Representative $[Ca^{2+}]_c$ oscillation responses are shown for ADP (A and B) and UTP (G and H).

(C–L) The frequency and width of the Ca^{2+} spikes induced by ADP and UTP were calculated from 5-min periods in the absence or presence of the PKC modulators. Summary data are shown for oscillation frequency and spike width (FWHM) for ADP (C–F) and UTP (I–L). See Figure S1 for the effect of staurosporine on the spike width of ADP- and UTP-induced $[Ca^{2+}]_c$ oscillations. Blue and green symbols represent data from ADP- and UTP-induced $[Ca^{2+}]_c$ oscillations, respectively. Data are mean ± S.E.M. from ≥50 cells from at least three independent experiments. ****, $p < 0.0001$; Student's t test.

that these receptors are functional in hepatocytes, including the activation of a Na^+-dependent inward current and Ca^{2+} influx in a rat hepatoma cell line (Emmett et al., 2008; Gonzales et al., 2007), and increased $[Ca^{2+}]_c$ and enhanced small molecule permeability in isolated rat hepatocytes (Emmett et al., 2008; Gonzales et al., 2007). In addition, the P2X4 receptor allosteric activator ivermectin also increases $[Ca^{2+}]_c$ in hepatoma cells (Emmett et al., 2008; Gonzales et al., 2007).

In primary rat hepatocytes, low doses of ATP (1–10 μM), the agonist for all P2 receptors, elicits $[Ca^{2+}]_c$ oscillations (Cobbold et al., 1991; Dixon et al., 1990, 2000). In the present study, we demonstrated that $[Ca^{2+}]_c$ responses elicited by physiological concentrations of extracellular ATP are blocked by a $G\alpha_q$ inhibitor, whereas the sustained monophasic $[Ca^{2+}]_c$ increases observed at high ATP concentrations are unaffected by $G\alpha_q$ inhibition. It seems likely that P2X7 receptor activity accounts for the latter monophasic $[Ca^{2+}]_c$ responses, since activation of this receptor has been shown to require higher ATP ($EC_{50} \geq 100$ μM) compared with other P2X receptors (Bianchi et al., 1999; Surprenant and North, 2009). In fact, Gonzalez and colleagues demonstrated previously that treatment with high ATP (1 mM) or BzATP (100–300 μM) induced membrane pore formation and blebbing in rat hepatocytes, and these events were inhibited by oxidized ATP, an antagonist of P2X7 receptors (Gonzales et al., 2007). However, since BzATP activates both P2X4 and P2X7 receptors (North, 2002), the pharmacological approach used here and in the previous study cannot distinguish unequivocally between the individual roles of these receptors in the sustained $[Ca^{2+}]_c$ increase in rat hepatocytes at high levels of ATP.

Summarizing the findings with respect to P2X receptors, although P2X4 and/or P2X7 are functional and able to increase $[Ca^{2+}]_c$ in rat hepatocytes, these receptors do not appear to play a role in the generation of $[Ca^{2+}]_c$ oscillations and, therefore, in the physiological liver functions mediated by these Ca^{2+} signals. Nevertheless, their activation by high ATP levels suggests a potential role of P2X purinergic signaling under pathophysiological conditions in liver. Indeed, a role of the P2X7 receptor in cytotoxicity and ATP-mediated apoptosis has been described in the liver (Fausther and Sevigny, 2011; Gonzales et al., 2007). Importantly, perfusion of rat liver with ATP, within the dose range shown in this study to induce oscillatory $[Ca^{2+}]_c$ responses (1–10 μM ATP), increases hepatic glucose output, indicating that P2Y receptors are responsible for stimulating glycogenolysis (Buxton et al., 1986).

In the present study, P2Y1 and P2Y2 receptor mRNA were the most abundantly expressed among the $G\alpha_q$-coupled P2Y receptors, in agreement with previous mRNA expression analysis from rat hepatocytes (Dixon et al., 2000). Although mRNA expression of P2Y6 receptors has been reported from non-quantitative PCR analysis (Dixon et al., 2000), our quantitative PCR data revealed only a low expression level of P2Y6 receptors compared to other P2Y subtypes. At the functional level, UDP, which is the most potent P2Y6 agonist (Nicholas et al., 1996), failed to elicit a $[Ca^{2+}]_c$ response, consistent with previous findings (Dixon et al., 2000). All of the other endogenous purinergic nucleotide agonists, ATP, ADP, and UTP, were able to elicit $[Ca^{2+}]_c$ oscillations in rat hepatocytes. In our studies, ATP was the only agonist able to evoke a response in 100% of hepatocytes. The inability of ADP and UTP to elicit a $[Ca^{2+}]_c$ response in all cells could be explained by different expression levels of P2Y1 and P2Y2 receptors, which would relate to heterogeneous distribution of these receptors through the liver, particularly along the zonal axis of the hepatic lobule.

The oscillatory $[Ca^{2+}]_c$ signaling induced by $G\alpha_q$-coupled receptors is well established to regulate hepatic metabolism (Exton, 1987; Gaspers et al., 2019; Hajnoczky et al., 1995). Furthermore, individual GPCRs elicit $[Ca^{2+}]_c$ oscillations with distinct Ca^{2+} spike kinetics, most notably in the falling phase, allowing for differential regulation of downstream targets (Bartlett et al., 2014; Dixon et al., 2000; Rooney et al., 1989). Several components of the Ca^{2+} signaling pathway have been described that modulate $[Ca^{2+}]_c$ oscillations and the profile of individual Ca^{2+} spikes via positive and negative feedback mechanisms. Positive feedback of $[Ca^{2+}]_c$ on PLC and consequent cross-coupling of Ca^{2+} and IP_3 is an essential component in the generation of $[Ca^{2+}]_c$ oscillations in hepatocytes (Gaspers et al., 2014; Politi et al., 2006; Bartlett et al., 2020). In addition, negative feedback by PKC on PLC-dependent IP_3 formation may play a role in spike termination, and in setting the frequency of hormone-induced $[Ca^{2+}]_c$ oscillations (Bartlett et al., 2015). The remarkably distinct Ca^{2+} spike profiles evoked by P2Y1 and P2Y2 receptors suggests that differential regulation of the Ca^{2+} mobilization machinery gives rise to receptor-specific differences in the duration and kinetics of the Ca^{2+} spike falling phase. This is unexpected, since all of the $G\alpha_q$-linked receptors, including P2Y1 and P2Y2 receptors, engage the same signaling machinery utilizing IP_3 to mobilize intracellular Ca^{2+} stores. The mechanism underlying distinct stereotypic Ca^{2+} spike profiles with different agonists has not previously been resolved.

The narrow Ca^{2+} spikes associated with P2Y1 receptor activation and the broad Ca^{2+} spikes associated with P2Y2 receptor activation are both altered by PKC modulation but with clear differences that contribute to the distinct Ca^{2+} spike profiles. Inhibition of PKC activity by PKC-DR increased the spike width in all cases, but this was much more pronounced for P2Y1 receptor. This PKC-DR approach has also been shown to enhance the oscillatory $[Ca^{2+}]_c$ responses to the α-adrenergic agonist phenylephrine in rat hepatocytes, again with a prolongation of the Ca^{2+} spike width (Bartlett et al., 2015). In those studies, we demonstrated that agonist-stimulated PLC activity and IP_3 production were enhanced due to the absence of negative feedback by PKC on the GPCR-dependent stimulation of PLC (Bartlett et al., 2015). Thus, the broadening of $[Ca^{2+}]_c$ oscillations observed for activation of P2Y1 and P2Y2 receptors are also likely due to the suppression of PKC negative feedback on IP_3 production, particularly during the falling phase of the individual Ca^{2+} spikes. We interpret this to suggest that under normal conditions there is a larger element of PKC negative feedback onto the P2Y1 as opposed to the P2Y2 receptors, such that PKC-DR has a much more pronounced effect to modulate the P2Y1 response to ADP. Consistent with this, PKC-DR shifted the $[Ca^{2+}]_c$ signature profile toward more oscillatory and sustained responses for ADP stimulation, but not for UTP stimulation (Figures 5E vs 5F). This indicates that there is a selective effect of PKC to suppress the strength of the $[Ca^{2+}]_c$ signals elicited by P2Y1 receptor activation, which is relieved by elimination of this negative feedback after PKC-DR.

The differential PKC-dependent feedback mechanism of P2Y1 and P2Y2 receptors was also evidenced by acute modulation of PKC. P2Y1 activation with ADP in the presence of the PKC inhibitor BIM led to broader $[Ca^{2+}]_c$ spike widths, consistent with the data obtained with PKC-DR. As discussed above, this can be explained by the elimination of PKC negative feedback on the P2Y1 receptor-stimulated PLC. By contrast, acute PKC activation with PMA did not further decrease the already narrow Ca^{2+} spikes with P2Y1 receptor activation but did slightly decrease the $[Ca^{2+}]_c$ oscillation frequency. These data are consistent with a strong endogenous negative feedback effect of PKC on P2Y1 receptors. As noted above, there was only a small effect of PKC-DR on P2Y2-induced $[Ca^{2+}]_c$ oscillations, suggesting that endogenous PKC-dependent negative feedback plays a lesser role than for the P2Y1 responses. Nevertheless, acute PKC activation with PMA caused a significant narrowing of UTP-induced $[Ca^{2+}]_c$ oscillations, demonstrating that P2Y2 receptor-mediated PLC activation is susceptible to PKC negative feedback, but this is not full engaged by the endogenous activation of PKC during UTP stimulation. The paradoxical finding that BIM also caused narrowing of the Ca^{2+} spike width in response to UTP stimulation could be explained by a discrete site of action, perhaps through a different PKC isozyme that is not susceptible to PKC-DR. One potential target is the IP_3R, which we have shown previously is sensitized to IP_3 by PKC activation but is unaffected by PKC-DR in hepatocytes (Bartlett et al., 2015). Thus, with P2Y1 receptor activation the predominant effect of PKC may be negative feedback on PLC-dependent IP_3 generation at the plasma membrane, whereas with P2Y2 receptor activation intracellular IP_3R sensitization by PKC may predominate.

Our findings with respect to the influence of extracellular Ca^{2+} on the shape of the $[Ca^{2+}]_c$ oscillations elicited by P2Y1 and P2Y2 receptor activation sheds light on the differential effects of PKC. Bearing in mind the importance of plasma membrane Ca^{2+} entry in maintaining $[Ca^{2+}]_c$ oscillations, the observation that the Ca^{2+} spikes elicited by ADP were substantially broader in the absence of extracellular Ca^{2+} was unexpected. Moreover, this effect was specific to P2Y1 receptor activation by ADP, and was not observed with UTP activation of P2Y2 receptors (Figure 6). The effect of extracellular Ca^{2+} to broaden the $[Ca^{2+}]_c$ spike width appears to be mediated by PKC, since there was no additional effect of Ca^{2+} removal in hepatocytes after PKC-DR. In other cell types there is evidence that extracellular Ca^{2+} is important for PKC activation, and Ca^{2+} influx may play a direct role in the translocation and activation of plasma membrane-associated conventional PKC isoforms (May et al., 2014; Rasmussen et al., 1995; Zhou et al., 2006). Our observation in hepatocytes that plasma membrane Ca^{2+} entry is required for negative PKC feedback only on ADP-induced $[Ca^{2+}]_c$ oscillations is consistent with the conclusion that PKC acts selectively on P2Y1 receptor signaling to shape the narrow Ca^{2+} spikes elicited by this receptor, whereas P2Y2 receptors signaling is refractory to this feedback. It is also significant because it provides evidence that plasma membrane Ca^{2+} entry can have discrete effects on PKC activation, distinct from the concomitant changes in bulk cytosolic Ca^{2+}.

From a broader perspective, these data indicate that multiple PKC isoforms with distinct Ca^{2+} signaling targets and different modes of activation are engaged to fine-tune agonist-induced $[Ca^{2+}]_c$ oscillations and to shape the Ca^{2+} spike kinetics for a given GPCR. Indeed, in human platelets, distinct PKC isoforms

have been shown to regulate P2Y1 and P2Y12 receptor function and trafficking. Overexpression of dominant-negative PKC-α and PKC-δ isoforms revealed both novel and conventional PKC-mediate P2Y1 desensitization, whereas only novel PKCs regulate P2Y12 receptors (Mundell et al., 2006). A differential susceptibility to PKC was described in human astrocyte cell line, in which stimulation of both P2Y1 and P2Y2 receptors elicited Ca^{2+} responses. However, high-frequency activation of P2Y1 receptors recruited a negative feedback mediated by PKC, which was not engaged by P2Y2 activation (Fam et al., 2003). The residue Thr_{339} in the C terminus of the P2Y1 receptor seems to be necessary for its downregulation by PKC (Fam et al., 2003).

Another possible PKC target in the control of IP_3 formation and Ca^{2+} mobilization is PLC. PKC-mediated phosphorylation of PLC-β3 (but not PLC-β1) in response to P2Y2 and M3 muscarinic receptor activation has been shown to decrease PLC association with $G\alpha_q/_{11}$ and contribute to the termination of the $[Ca^{2+}]_c$ increases evoked by these receptors (Strassheim and Williams, 2000). This type of negative feedback on PLC activity could explain the effects of PKC on Ca^{2+} spike duration observed in the present work. PKC activity can also regulate the degradation of IP_3. In fibroblast cell lines, PKC phosphorylates IP_3 Kinase isoforms A and B, decreasing the Ca^{2+}/calmodulin-stimulated activity (Woodring and Garrison, 1997), thereby slowing the removal of IP_3. However, this would not explain our findings with P2Y1 receptors, where PKC activity is associated with shorter duration Ca^{2+} spikes. By contrast, in platelets PKC activates IP_3 5-phosphatase, increasing the rate of IP_3 degradation (Connolly et al., 1986), and inhibition with staurosporine increases IP_3 accumulation (King and Rittenhouse, 1989). Thus, the prolonged Ca^{2+} spikes seen with P2Y1 receptor activation after PKC-DR or acute PKC inhibition could be explained by lack of IP_3 5-phosphatase activation, although it is more difficult to see how this would result in a differential effect on P2Y1 vs P2Y2 receptors. Finally, the IP_3R Ca^{2+} channel itself appears to be a PKC target. We have shown that the frequency of $[Ca^{2+}]_c$ oscillations elicited by uncaging IP_3 in hepatocytes is increased by acute PMA treatment, indicating that IP_3-induced Ca^{2+} release may also be directly enhanced by PKC (Bartlett et al., 2015).

Overall, these multiple actions of PKC, and perhaps others, contribute to regulate the frequency and individual spike dynamics of agonist-induced $[Ca^{2+}]_c$ oscillations. The present findings showing how these feedback mechanisms mediated by PKC can give rise to distinct receptor-specific shaping of $[Ca^{2+}]_c$ oscillations, even within the P2Y $G\alpha_q$-linked GPCR family, provides the first complete explanation of the remarkable observations that different hormones give rise to characteristic $[Ca^{2+}]_c$ oscillation shapes reported by Cobbold and coworkers and our group more than 30 years ago (Woods et al., 1986; Rooney et al., 1989; Sanchez-Bueno and Cobbold, 1993). In the context of liver function and hepatology, the ability to generate distinct Ca^{2+} signaling patterns allows different receptors to exert control over specific hepatocyte functions. For example, brief Ca^{2+} spikes can acutely activate cytosolic metabolism, including glycogenolysis, whereas longer duration Ca^{2+} spikes may be important for mitochondrial activation, lipid metabolism and gene expression, and the complex patterns of response to ATP may underlie its broader range of actions including in liver regeneration (Bartlett et al., 2014; Burnstock et al., 2014; Kimura et al., 2020).

In conclusion, our results show that P2Y1 and P2Y2 receptors are functional and display stereotypic $[Ca^{2+}]_c$ oscillations that are tightly regulated by PKC feedback mechanisms in primary rat hepatocytes. P2Y1 receptor-evoked $[Ca^{2+}]_c$ oscillations are shaped by a strong negative feedback on PLC activation, with a key role of plasma membrane Ca^{2+} entry in this component of PKC action. The distinct $[Ca^{2+}]_c$ oscillation pattern seen with P2Y2 receptor activation appears to involve differential regulation by PKC, reflecting differences in the sensitivity of IP_3 generation and downstream components of IP_3 metabolism and action in the Ca^{2+} signaling cascade. The P2Y receptor-specific $[Ca^{2+}]_c$ signatures established by PKC in the liver provide a means to regulate the diverse targets, including both physiological and pathophysiological processes, all encoded by the complex $[Ca^{2+}]_c$ oscillation signals.

Limitations of the study

Hepatocytes were one of the first cell types to be shown to manifest $[Ca^{2+}]_c$ oscillations in the continuing presence of agonist, and they remain one of the best examples where the agonist controls the frequency, but not the amplitude, of baseline-separate periodic Ca^{2+} spikes. Similar $[Ca^{2+}]_c$ oscillations are seen in many other primary cell types and tissues, especially in epithelial and secretory cells, where agonist-specific Ca^{2+} spike shapes are also observed. However, more chaotic $[Ca^{2+}]_c$ oscillations are observed in other cell types, especially cell lines maintained in long-term culture, and cell polarization may be a factor in these

differences. As polarized epithelial cells, there may be a morphological component to the organization that gives rise to stereotypic Ca^{2+} spikes in hepatocytes, which would be difficult to resolve using currently available tools for studying IP_3-related signaling components. We focused our studies on two closely related purinergic P2Y receptors, which presents a good paradigm for studying the differential regulation of GPCR-mediated $[Ca^{2+}]_c$ oscillations because despite their similarities they yield remarkably different Ca^{2+} response patterns. Nevertheless, other GPCRs also show stereotypic Ca^{2+} spikes in hepatocytes and future work should investigate whether similar mechanisms are more broadly applicable. Finally, although we show receptor-specific regulation by PKC feedback underlies the distinct $[Ca^{2+}]_c$ oscillations patterns, we do not have the tools to elucidate the precise sites of PKC action. While it could act directly on the specific GPCRs involved, PKC could also act on other coupling proteins or auxiliary proteins associated with the GPCR/PLC signaling cascade. Moreover, the differential actions of PKC might reflect the subcellular localization or targeting of PKC to the relevant signaling complex rather than a receptor-specific target in the polarized hepatocytes.

STAR★ METHODS

Detailed methods are provided in the online version of this paper and include the following:

- KEY RESOURCES TABLE
- RESOURCE AVAILABILITY
  - Lead contact
  - Materials availability
  - Data and code availability
- EXPERIMENTAL MODEL AND SUBJECT DETAILS
  - Animals
  - Primary cell culture
- METHOD DETAILS
  - RNA extraction and cDNA synthesis
  - Quantitative PCR
  - Cytosolic Ca^{2+} measurements
- QUANTIFICATION AND STATISTICAL ANALYSIS
  - Data analysis

SUPPLEMENTAL INFORMATION

Supplemental information can be found online at https://doi.org/10.1016/j.isci.2021.103139.

ACKNOWLEDGMENTS

This work was supported by the Thomas P. Infusino Endowment and NIH R01DK078019. H.U. acknowledges grant support from the São Paulo Research Foundation (FAPESP 2018/07366-4) and fellowship support from CNPq (CNPq 306392/2017-8).

AUTHOR CONTRIBUTIONS

A.P.T., P.J.B., L.D.G., and J.C.C.-V. designed the research; J.C.C.-V. performed the research and analyzed the data; R.B. designed the analysis algorithm; H.U. and A.P.T provided funding acquisitions and resources; J.C.C.-V., P.J.B., and A.P.T. wrote the manuscript.

DECLARATION OF INTEREST

The authors declare no competing interests.

INCLUSION AND DIVERSITY

One or more of the authors of this paper self-identifies as an underrepresented ethnic minority in science.

Received: April 26, 2021
Revised: July 26, 2021
Accepted: September 14, 2021
Published: October 22, 2021

REFERENCES

Abbracchio, M.P., Burnstock, G., Boeynaems, J.M., Barnard, E.A., Boyer, J.L., Kennedy, C., Knight, G.E., Fumagalli, M., Gachet, C., Jacobson, K.A., and Weisman, G.A. (2006). International Union of Pharmacology LVIII: update on the P2Y G protein-coupled nucleotide receptors: from molecular mechanisms and pathophysiology to therapy. Pharmacol. Rev. *58*, 281–341.

Barrera, N.P., Ormond, S.J., Henderson, R.M., Murrell-Lagnado, R.D., and Edwardson, J.M. (2005). Atomic force microscopy imaging demonstrates that P2X2 receptors are trimers but that P2X6 receptor subunits do not oligomerize. J. Biol. Chem. *280*, 10759–10765.

Bartlett, P.J., Cloete, I., Sneyd, J., and Thomas, A.P. (2020). IP3-Dependent Ca(2+) oscillations switch into a dual oscillator mechanism in the presence of PLC-linked hormones. iScience *23*, 101062.

Bartlett, P.J., Gaspers, L.D., Pierobon, N., and Thomas, A.P. (2014). Calcium-dependent regulation of glucose homeostasis in the liver. Cell Calcium *55*, 306–316.

Bartlett, P.J., Metzger, W., Gaspers, L.D., and Thomas, A.P. (2015). Differential regulation of multiple steps in inositol 1,4,5-trisphosphate signaling by protein kinase C shapes hormone-stimulated Ca^{2+} oscillations. J. Biol. Chem. *290*, 18519–18533.

Beldi, G., Enjyoji, K., Wu, Y., Miller, L., Banz, Y., Sun, X., and Robson, S.C. (2008). The role of purinergic signaling in the liver and in transplantation: effects of extracellular nucleotides on hepatic graft vascular injury, rejection and metabolism. Front. Biosci. *13*, 2588–2603.

Berridge, M.J., Bootman, M.D., and Roderick, H.L. (2003). Calcium signalling: dynamics, homeostasis and remodelling. Nat. Rev. Mol. Cell Biol *4*, 517–529.

Berrie, C.P., and Cobbold, P.H. (1995). Both activators and inhibitors of protein kinase C promote the inhibition of phenylephrine-induced $[Ca^{2+}]i$ oscillations in single intact rat hepatocytes. Cell Calcium *18*, 232–244.

Bianchi, B.R., Lynch, K.J., Touma, E., Niforatos, W., Burgard, E.C., Alexander, K.M., Park, H.S., Yu, H., Metzger, R., Kowaluk, E., et al. (1999). Pharmacological characterization of recombinant human and rat P2X receptor subtypes. Eur. J. Pharmacol. *376*, 127–138.

Bogdanov, Y.D., Wildman, S.S., Clements, M.P., King, B.F., and Burnstock, G. (1998). Molecular cloning and characterization of rat P2Y4 nucleotide receptor. Br. J. Pharmacol. *124*, 428–430.

Burnstock, G., Vaughn, B., and Robson, S.C. (2014). Purinergic signalling in the liver in health and disease. Purinergic Signal *10*, 51–70.

Buxton, D.B., Robertson, S.M., and Olson, M.S. (1986). Stimulation of glycogenolysis by adenine nucleotides in the perfused rat liver. Biochem. J. *237*, 773–780.

Chiavegatto, S., Izidio, G.S., Mendes-Lana, A., Aneas, I., Freitas, T.A., Torrao, A.S., Conceicao, I.M., Britto, L.R., and Ramos, A. (2009). Expression of alpha-synuclein is increased in the hippocampus of rats with high levels of innate anxiety. Mol. Psychiatry *14*, 894–905.

Clapham, D.E. (2007). Calcium signaling. Cell *131*, 1047–1058.

Cobbold, P.H., Sanchez-Bueno, A., and Dixon, C.J. (1991). The hepatocyte calcium oscillator. Cell Calcium *12*, 87–95.

Connolly, T.M., Lawing, W.J., Jr., and Majerus, P.W. (1986). Protein kinase C phosphorylates human platelet inositol trisphosphate 5'-phosphomonoesterase, increasing the phosphatase activity. Cell *46*, 951–958.

Dixon, C.J., Cobbold, P.H., and Green, A.K. (1993). Adenosine 5'-[alpha beta-methylene] triphosphate potentiates the oscillatory cytosolic Ca^{2+} responses of hepatocytes to ATP, but not to ADP. Biochem. J. *293*, 757–760.

Dixon, C.J., Cobbold, P.H., and Green, A.K. (1995). Actions of ADP, but not ATP, on cytosolic free Ca^{2+} in single rat hepatocytes mimicked by 2-methylthioATP. Br. J. Pharmacol. *116*, 1979–1984.

Dixon, C.J., Hall, J.F., and Boarder, M.R. (2003). ADP stimulation of inositol phosphates in hepatocytes: role of conversion to ATP and stimulation of P2Y2 receptors. Br. J. Pharmacol. *138*, 272–278.

Dixon, C.J., Hall, J.F., Webb, T.E., and Boarder, M.R. (2004). Regulation of rat hepatocyte function by P2Y receptors: focus on control of glycogen phosphorylase and cyclic AMP by 2-methylthioadenosine 5'-diphosphate. J. Pharmacol. Exp. Ther. *311*, 334–341.

Dixon, C.J., White, P.J., Hall, J.F., Kingston, S., and Boarder, M.R. (2005). Regulation of human hepatocytes by P2Y receptors: control of glycogen phosphorylase, Ca^{2+}, and mitogen-activated protein kinases. J. Pharmacol. Exp. Ther. *313*, 1305–1313.

Dixon, C.J., Woods, N.M., Cuthbertson, K.S., and Cobbold, P.H. (1990). Evidence for two Ca2(+)-mobilizing purinoceptors on rat hepatocytes. Biochem. J. *269*, 499–502.

Dixon, C.J., Woods, N.M., WEBB, T.E., and GREEN, A.K. (2000). Evidence that rat hepatocytes co-express functional P2Y1 and P2Y2 receptors. Br. J. Pharmacol. *129*, 764–770.

Dlugosz, A.A., and Yuspa, S.H. (1991). Staurosporine induces protein kinase C agonist effects and maturation of normal and neoplastic mouse keratinocytes in vitro. Cancer Res. *51*, 4677–4684.

Doctor, R.B., Matzakos, T., Mcwilliams, R., Johnson, S., Feranchak, A.P., and Fitz, J.G. (2005). Purinergic regulation of cholangiocyte secretion: identification of a novel role for P2X receptors. Am. J. Physiol. Gastrointest. Liver Physiol. *288*, G779–G786.

Emmett, D.S., Feranchak, A., Kilic, G., Puljak, L., Miller, B., Dolovcak, S., Mcwilliams, R., Doctor, R.B., and FITZ, J.G. (2008). Characterization of ionotrophic purinergic receptors in hepatocytes. Hepatology *47*, 698–705.

Erb, L., and Weisman, G.A. (2012). Coupling of P2Y receptors to G proteins and other signaling pathways. Wiley Interdiscip. Rev. Membr. Transp. Signal *1*, 789–803.

Exton, J.H. (1987). Mechanisms of hormonal regulation of hepatic glucose metabolism. Diabetes Metab. Rev. *3*, 163–183.

Fam, S.R., Gallagher, C.J., Kalia, L.V., and Salter, M.W. (2003). Differential frequency dependence of P2Y1- and P2Y2- mediated Ca^{2+} signaling in astrocytes. J. Neurosci. *23*, 4437–4444.

Fausther, M., and Sevigny, J. (2011). Extracellular nucleosides and nucleotides regulate liver functions via a complex system of membrane proteins. C. R. Biol. *334*, 100–117.

Fitz, J.G. (2007). Regulation of cellular ATP release. Trans. Am. Clin. Climatol Assoc. *118*, 199–208.

Gaspers, L.D., Bartlett, P.J., Politi, A., Burnett, P., Metzger, W., Johnston, J., Joseph, S.K., Hofer, T., and Thomas, A.P. (2014). Hormone-induced calcium oscillations depend on cross-coupling with inositol 1,4,5-trisphosphate oscillations. Cell Rep. *9*, 1209–1218.

Gaspers, L.D., Pierobon, N., and Thomas, A.P. (2019). Intercellular calcium waves integrate hormonal control of glucose output in the intact liver. J. Physiol. *597*, 2867–2885.

Gaspers, L.D., and Thomas, A.P. (2005). Calcium signaling in liver. Cell Calcium *38*, 329–342.

Glaser, T., de Oliveira, S.L., Cheffer, A., Beco, R., Martins, P., Fornazari, M., Lameu, C., Junior, H.M., Coutinho-Silva, R., and Ulrich, H. (2014). Modulation of mouse embryonic stem cell proliferation and neural differentiation by the P2X7 receptor. PLoS One *9*, e96281.

Gonzales, E., Julien, B., Serriere-Lanneau, V., Nicou, A., Doignon, I., Lagoudakis, L., Garcin, I., Azoulay, D., Duclos-Vallee, J.C., Castaing, D., et al. (2010). ATP release after partial hepatectomy regulates liver regeneration in the rat. J. Hepatol. *52*, 54–62.

Gonzales, E., Prigent, S., Abou-Lovergne, A., Boucherie, S., Tordjmann, T., Jacquemin, E., and Combettes, L. (2007). Rat hepatocytes express functional P2X receptors. FEBS Lett. *581*, 3260–3266.

Green, A.K., Cobbold, P.H., and Dixon, C.J. (1994). Elevated intracellular cyclic AMP exerts different modulatory effects on cytosolic free Ca^{2+} oscillations induced by ADP and ATP in single rat hepatocytes. Biochem. J. *302*, 949–955.

Hajnoczky, G., Robb-Gaspers, L.D., Seitz, M.B., and Thomas, A.P. (1995). Decoding of cytosolic calcium oscillations in the mitochondria. Cell *82*, 415–424.

Hajnoczky, G., and Thomas, A.P. (1997). Minimal requirements for calcium oscillations driven by the IP3 receptor. EMBO J. *16*, 3533–3543.

Kennedy, C. (2017). P2Y11 receptors: properties, distribution and functions. Adv. Exp. Med. Biol. *1051*, 107–122.

Kimura, T., Pydi, S.P., Pham, J., and Tanaka, N. (2020). Metabolic functions of G protein-coupled receptors in hepatocytes-potential applications for diabetes and NAFLD. Biomolecules *10*, 1445.

King, W.G., and Rittenhouse, S.E. (1989). Inhibition of protein kinase C by staurosporine promotes elevated accumulations of inositol trisphosphates and tetrakisphosphate in human platelets exposed to thrombin. J. Biol. Chem. *264*, 6070–6074.

Lagoudakis, L., Garcin, I., Julien, B., Nahum, K., Gomes, D.A., Combettes, L., Nathanson, M.H., and Tordjmann, T. (2010). Cytosolic calcium regulates liver regeneration in the rat. Hepatology *52*, 602–611.

May, V., Clason, T.A., Buttolph, T.R., Girard, B.M., and Parsons, R.L. (2014). Calcium influx, but not intracellular calcium release, supports PACAP-mediated ERK activation in HEK PAC1 receptor cells. J. Mol. Neurosci. *54*, 342–350.

Mundell, S.J., Jones, M.L., Hardy, A.R., Barton, J.F., Beaucourt, S.M., CONLEY, P.B., and POOLE, A.W. (2006). Distinct roles for protein kinase C isoforms in regulating platelet purinergic receptor function. Mol. Pharmacol. *70*, 1132–1142.

Nicholas, R.A., Watt, W.C., Lazarowski, E.R., Li, Q., and Harden, K. (1996). Uridine nucleotide selectivity of three phospholipase C-activating P2 receptors: identification of a UDP-selective, a UTP-selective, and an ATP- and UTP-specific receptor. Mol. Pharmacol. *50*, 224–229.

North, R.A. (2002). Molecular physiology of P2X receptors. Physiol. Rev. *82*, 1013–1067.

Ohtomo, K., Shatos, M.A., Vrouvlianis, J., LI, D., Hodges, R.R., and Dartt, D.A. (2011). Increase of intracellular Ca^{2+} by purinergic receptors in cultured rat lacrimal gland myoepithelial cells. Invest. Ophthalmol. Vis. Sci. *52*, 9503–9515.

Patel, S., Joseph, S.K., and Thomas, A.P. (1999). Molecular properties of inositol 1,4,5-trisphosphate receptors. Cell Calcium *25*, 247–264.

Politi, A., Gaspers, L.D., Thomas, A.P., and Hofer, T. (2006). Models of IP3 and Ca^{2+} oscillations: frequency encoding and identification of underlying feedbacks. Biophys. J. *90*, 3120–3133.

Ralevic, V., and Burnstock, G. (1998). Receptors for purines and pyrimidines. Pharmacol. Rev. *50*, 413–492.

Rasmussen, H., Isales, C.M., Calle, R., Throckmorton, D., Anderson, M., Gasalla-Herraiz, J., and Mccarthy, R. (1995). Diacylglycerol production, Ca^{2+} influx, and protein kinase C activation in sustained cellular responses. Endocr. Rev. *16*, 649–681.

Robb-Gaspers, L.D., and Thomas, A.P. (1995). Coordination of Ca^{2+} signaling by intercellular propagation of Ca^{2+} waves in the intact liver. J. Biol. Chem. *270*, 8102–8107.

Rooney, T.A., Sass, E.J., and Thomas, A.P. (1989). Characterization of cytosolic calcium oscillations induced by phenylephrine and vasopressin in single fura-2-loaded hepatocytes. J. Biol. Chem. *264*, 17131–17141.

Sanchez-Bueno, A., and Cobbold, P.H. (1993). Agonist-specificity in the role of Ca(2+)-induced Ca^{2+} release in hepatocyte Ca^{2+} oscillations. Biochem. J. *291*, 169–172.

Sanchez-Bueno, A., Dixon, C.J., Woods, N.M., Cuthbertson, K.S., and Cobbold, P.H. (1990). Inhibitors of protein kinase C prolong the falling phase of each free-calcium transient in a hormone-stimulated hepatocyte. Biochem. J. *268*, 627–632.

Schakel, L., Schmies, C.C., Idris, R.M., Luo, X., LEE, S.Y., Lopez, V., Mirza, S., Vu, T.H., Pelletier, J., Sevigny, J., et al. (2020). Nucleotide analog ARL67156 as a lead structure for the development of CD39 and dual CD39/CD73 ectonucleotidase inhibitors. Front. Pharmacol. *11*, 1294.

Schlosser, S.F., Burgstahler, A.D., and Nathanson, M.H. (1996). Isolated rat hepatocytes can signal to other hepatocytes and bile duct cells by release of nucleotides. Proc. Natl. Acad. Sci. U. S. A. *93*, 9948–9953.

Schofl, C., Ponczek, M., Mader, T., Waring, M., Benecke, H., von Zur Muhlen, A., Mix, H., Cornberg, M., Boker, K.H., Manns, M.P., and Wagner, S. (1999). Regulation of cytosolic free calcium concentration by extracellular nucleotides in human hepatocytes. Am. J. Physiol. *276*, G164–G172.

Steinberg, S.F. (2008). Structural basis of protein kinase C isoform function. Physiol. Rev. *88*, 1341–1378.

Strassheim, D., and Williams, C.L. (2000). P2Y2 purinergic and M3 muscarinic acetylcholine receptors activate different phospholipase C-beta isoforms that are uniquely susceptible to protein kinase C-dependent phosphorylation and inactivation. J. Biol. Chem. *275*, 39767–39772.

Surprenant, A., and North, R.A. (2009). Signaling at purinergic P2X receptors. Annu. Rev. Physiol. *71*, 333–359.

Tackett, B.C., Sun, H., Mei, Y., Maynard, J.P., Cheruvu, S., Mani, A., Hernandez-Garcia, A., Vigneswaran, N., Karpen, S.J., and Thevananther, S. (2014). P2Y2 purinergic receptor activation is essential for efficient hepatocyte proliferation in response to partial hepatectomy. Am. J. Physiol. Gastrointest. Liver Physiol. *307*, G1073–G1087.

Tatsushima, K., Hasuzawa, N., Wang, L., Hiasa, M., Sakamoto, S., Ashida, K., Sudo, N., Moriyama, Y., and Nomura, M. (2021). Vesicular ATP release from hepatocytes plays a role in the progression of nonalcoholic steatohepatitis. Biochim. Biophys. Acta Mol. Basis Dis. *1867*, 166013.

Thevananther, S., Sun, H., Li, D., Arjunan, V., Awad, S.S., Wyllie, S., Zimmerman, T.L., Goss, J.A., and Karpen, S.J. (2004). Extracellular ATP activates c-jun N-terminal kinase signaling and cell cycle progression in hepatocytes. Hepatology *39*, 393–402.

Thomas, A.P., Renard, D.C., and Rooney, T.A. (1991). Spatial and temporal organization of calcium signalling in hepatocytes. Cell Calcium *12*, 111–126.

Trefts, E., Gannon, M., and Wasserman, D.H. (2017). The liver. Curr. Biol. *27*, R1147–R1151.

Uemura, T., Kawasaki, T., Taniguchi, M., Moritani, Y., Hayashi, K., Saito, T., Takasaki, J., Uchida, W., and Miyata, K. (2006). Biological properties of a specific Galpha q/11 inhibitor, YM-254890, on platelet functions and thrombus formation under high-shear stress. Br. J. Pharmacol. *148*, 61–69.

Vandesompele, J., de Preter, K., Pattyn, F., Poppe, B., VAN ROY, N., DE PAEPE, A., and SPELEMAN, F. (2002). Accurate normalization of real-time quantitative RT-PCR data by geometric averaging of multiple internal control genes. Genome Biol. *3*, 1–12.

Vaughn, B.P., Robson, S.C., and Burnstock, G. (2012). Pathological roles of purinergic signaling in the liver. J. Hepatol. *57*, 916–920.

Vaughn, B.P., Robson, S.C., and Longhi, M.S. (2014). Purinergic signaling in liver disease. Dig. Dis. *32*, 516–524.

Vilborg, A., Passarelli, M.C., and Steitz, J.A. (2016). Calcium signaling and transcription: elongation, DoGs, and eRNAs. Receptors Clin. Investig. *3*, e1169.

Webb, T.E., Henderson, D.J., Roberts, J.A., and Barnard, E.A. (1998). Molecular cloning and characterization of the rat P2Y4 receptor. J. Neurochem. *71*, 1348–1357.

Woodring, P.J., and Garrison, J.C. (1997). Expression, purification, and regulation of two isoforms of the inositol 1,4,5-trisphosphate 3-kinase. J. Biol. Chem. *272*, 30447–30454.

Woods, N.M., Cuthbertson, K.S., and Cobbold, P.H. (1986). Repetitive transient rises in cytoplasmic free calcium in hormone-stimulated hepatocytes. Nature *319*, 600–602.

Zeng, L., Webster, S.V., and Newton, P.M. (2012). The biology of protein kinase C. Adv. Exp. Med. Biol. *740*, 639–661.

Zhou, X., Yang, W., and Li, J. (2006). Ca^{2+}- and protein kinase C-dependent signaling pathway for nuclear factor-kappaB activation, inducible nitric-oxide synthase expression, and tumor necrosis factor-alpha production in lipopolysaccharide-stimulated rat peritoneal macrophages. J. Biol. Chem. *281*, 31337–31347.

STAR★ METHODS

KEY RESOURCES TABLE

REAGENT or RESOURCE	SOURCE	IDENTIFIER
Chemicals, peptides, and recombinant proteins		
TRIzol	Thermo Fisher Scientific	Cat#: 15596026
DNAse I	Qiagen	Cat#: 79254
SYBR Green PCR Master Mix	Thermo Fisher Scientific	Cat#: 4309155
Collagen type I (rat tail protein)	Thermo Fisher Scientific	Cat# : 354236
William's E Medium	Thermo Fisher Scientific	Cat# : 12551-032
Insulin	Thermo Fisher Scientific	Cat#: 12585-014
Glutamine	Thermo Fisher Scientific	Cat#: 25030081
Penicillin/Streptomycin 10K/10K	Lonza	Cat#: 17-602E
Gentamycin	Sigma	Cat#: G1397
Fetal bovine serum	Gemini Bio-Products	Cat#: 900-208
Sulfobromophthalein	Fluka	Cat#: 18360
Probenecid	TCI Chemicals	Cat#: P1975
Fura-2 AM	ION Biosciences	Cat#: 1051B
Adenosine 5′-triphosphate disodium salt (ATP)	Tocris	Cat#: 3245
Adenosine 5′-diphosphate sodium salt (ADP)	Sigma	Cat#: A2754
Uridine-5′-triphosphate trisodium salt (UTP)	Alfa Aesar	Cat#: J63427-MC
Uridine 5′-diphosphate disodium salt (UDP)	Sigma	Cat#: 94330
Phorbol 12-myristate 13-acetate (PMA)	Cayman Chemical	Cat#: 10008014
Bisindolylmaleimide I (BIM)	Millipore	Cat#: 203290
Staurosporine	Alexis Biochemicals	Cat#: 380-014-M001
MRS 2500 tetraammonium salt	Tocris	Cat#: 2159
AR-C 118925XX	Tocris	Cat#: 4890
ARL 67156 trisodium salt	Tocris	Cat#: 1283
Critical commercial assays		
Superscript™ III First-Strand Synthesis System	Thermo Fisher Scientific	Cat#: 18080051
Experimental models: Organisms/strains		
Sprague-Dawley Male Rats	Taconic	NTac:SD Male
Oligonucleotides		
P2x1: Forward: 5′-CAGTTCCACGGACTGTAT-3′ Reverse: 5′-GAATCCCAAACACCGTGAA-3′	This paper	N/A
P2x2: Forward: 5′-TGCCTCCTCAGGCTACAACT-3′ Reverse: 5′- AGTGGTGGTAGTGCCGTTT-3′	This paper	N/A
P2x3: Forward: 5′- CTGCCTAACCTCACCGACAAG-3′ Reverse: 5′-AATACCCAGAACGCCACCC-3′	This paper	N/A
P2x4: Forward: 5′-CTCATCCGCAGCCGTAAAGT-3′ Reverse: 5′-TTTTCCCACACGAACACCCA- 3′	This paper	N/A

(*Continued on next page*)

Continued

REAGENT or RESOURCE	SOURCE	IDENTIFIER
P2x5: Forward: 5′-GGATGCCAATGTTGAGGTTG-3′ Reverse: 5′-TCCTGACGAACCCTCTCCAG- 3′	This paper	N/A
P2x6: Forward: 5′-CCCAGAGCATCCTTCTGTTCC-3′ Reverse: 5′-GGCACCAGCTCCAGATCTCA- 3′	This paper	N/A
P2x7: Forward: 5′-GGGAGGTGGTTCAGTGGGTAA-3′ Reverse: 5′- GGATGCTGTGATCCCAACAAA-3′	This paper	N/A
P2y1: Forward: 5′-GTCAGTGTGCTGGTATGGCT-3′ Reverse: 5′-TTTTCCGAATCCCAGTGCCA-3′	This paper	N/A
P2y2: Forward: 5′-TCAAACCGGCTTATGGGACC-3′ Reverse: 5′-GGAAAGGCAGGAAGCAGAG-3′	This paper	N/A
P2y4: Forward: 5′-CGGCGACTGTATCGACCTTT-3′ Reverse: 5′- TTGTGCGGGTGATGTGGAA-3′	This paper	N/A
P2y6: Forward: 5′-CAGGATGTCTGCTGGAACCT-3′ Reverse: 5′-CCCTCTCAGCCTCAAGCTAC-3′	This paper	N/A
P2y12: Forward: 5′-AACGCCTGCCTTGATCCATT-3′ Reverse: 5′-TACATTGGGGTCTCCTCGCT-3′	This paper	N/A
P2y13: Forward: 5′-CCGTGAAGAAATGTGCGTCC-3′ Reverse: 5′-TGAACTGGCATGTGTGACTGA-3′	This paper	N/A
P2y14: Forward: 5′-GGTGGGTTTCGCCTCATGT-3′ Reverse: 5′-CCTCAGGTGACCGGCATCT-3′	This paper	N/A
Rpl0 Forward: 5′-CTCGCTTCCTAGAGGGTGTCCGC-3′ Reverse: 5′- CTCCACAGACAAAGCCAGGAC-3′	This paper	N/A
Software and algorithms		
GraphPad Prism	GraphPad	https://www.graphpad.com/scientific-software/prism/
MATLAB software	MathWorks	https://www.mathworks.com/products/matlab.html

RESOURCE AVAILABILITY

Lead contact

Further information and requests for resources and reagents should be directed to and will be fulfilled by the lead contact, Andrew Thomas, New Jersey Medical School Rutgers, The State University of New Jersey (andrew.thomas@rutgers.edu).

Materials availability

This study did not generate new unique reagents.

Data and code availability

- All data produced or analyzed for this study are included in the published article and its supplementary information files.

- This paper does not report original code.
- Any additional information required to reanalyze the data reported in this paper is available from the lead contact upon request.

EXPERIMENTAL MODEL AND SUBJECT DETAILS

Animals

Animal studies were approved by the Institutional Animal Care and Use Committee at Rutgers, New Jersey Medical School. Male Sprague–Dawley rats (weighing 200–250 g; Taconic Biosciences, Rensselaer, NY, USA) were housed in ventilated cages under a 12:12 h dark /light cycle. Rats were given *ad libitum* access to rodent chow and water until the day of experiment. Rats were anaesthetized with an I.P. injection of pentobarbital (60 mg/kg) diluted 1:1 with PBS and vital signs were monitored throughout the procedure. The depth of anesthesia was assessed by relaxation of muscle tone and a loss of reflex responses to external stimuli.

Primary cell culture

Hepatocytes were isolated by a two-step collagenase perfusion of livers as previously described (Rooney et al., 1989; Thomas et al., 1991). Cell viability was determined by Trypan blue exclusion and typically ranged between 85 and 95%. Hepatocytes (7×10^5) were plated on collagen-coated (type I rat tail, Corning; 10 μg/cm^2) glass coverslips in William's E Medium (Thermo Fisher Scientific) supplemented, 2 mM glutamine, 10 units/ml penicillin (Lonza), 10 μg/ml streptomycin (Lonza) and 50 μg/ml gentamycin (Sigma). Overnight cultured hepatocytes were supplemented with 5% (v/v) fetal bovine serum (Gemini Bio-Products), 140 nM insulin (Thermo Fisher Scientific) for 3 hours and cultured overnight in 14nM insulin. Cells were maintained in a humidified atmosphere of 5% CO_2 and 95% air at 37°C.

METHOD DETAILS

RNA extraction and cDNA synthesis

Total RNA was isolated from hepatocytes using TRIzol reagent and followed by column purification (Qiagen), according to the manufacturer protocol. DNAse I treatment (Ampgrade, 1U/μg of RNA, Thermo Fisher Scientific) was performed for 15 min at room temperature to prevent residual DNA contamination. RNA was quantified by spectrophotometry (NanoDrop, Thermo Fisher Scientific). Two micrograms of DNAse-treated RNA of each sample were simultaneously reverse transcribed using Superscript™ III First-Strand Synthesis System (Thermo Fisher Scientific) according to the manufacturer protocol. After cDNA synthesis, samples were submitted to a 20-minute digestion with RNAseH at 37° C.

Quantitative PCR

Quantitative transcript analyses were performed in a StepOnePlus™ Real-Time PCR System (Thermo Fisher Scientific), as described previously (Glaser et al., 2014). Optimal conditions were obtained using a five-point, two-fold cDNA and primer dilution curve for each amplicom. Each qPCR reaction contained 12.5 ng of reversely transcribed RNA, each specific primer at 200 nM (Table S1) and SYBR Green PCR Master Mix (Thermo Fisher Scientific), following the manufacturer conditions. Samples with no DNA or with RNA (no reverse transcription) were included as negative controls. A dissociation curve was acquired to confirm product specificity and the absence of primer dimers. Relative transcript amount quantification was calculated from three technical replicates, as previously described (Chiavegatto et al., 2009; Vandesompele et al., 2002). Purinergic receptor gene expression was normalized to *Rpl0* expression, which did not change under the used experimental conditions.

Cytosolic Ca^{2+} measurements

Calcium imaging experiments were performed in HEPES-buffered physiological saline solution comprised of 25 mM HEPES (pH 7.4), 121 mM NaCl, 5 mM $NaHCO_3$, 10 mM glucose, 4.7 mM KCl, 1.2 mM KH_2PO_4, 1.2 mM $MgSO_4$, 1.3 mM $CaCl_2$, and 0.25%(w/v) fatty acid-free BSA and supplemented with the organic anion transport inhibitors sulfobromophthalein (100 μM) or probenecid (200 μM) to increase retention of fura-2. Hepatocytes were loaded with fura-2 by incubation with 5 μM fura-2/AM and Pluronic acid F-127 (0.02% v/v) for 20–40 min. Cells were transferred to a thermostatically regulated microscope chamber (37° C). Fura-2 fluorescence images (excitation, 340 and 380 nm, emission 510 nm long pass) were acquired

at 1 to 3 s intervals with a cooled charge-coupled device camera coupled to an epifluorescent microscope, as described previously (Hajnoczky and Thomas, 1997).

QUANTIFICATION AND STATISTICAL ANALYSIS

Data analysis

Relative expression of purinergic receptors genes was calculated according to Chiavegatto et al. (2009). Briefly, the arithmetic means of replicated cycling threshold (Cq) value of each gene was transformed to a quantity taking into account the amplification efficiency of each gene. The raw quantities were subsequently normalized to the reference gene. For the imaging data, the frequency and spike width (full width at half maximum, FWHM), were determined using algorithms (R.B. et al., unpublished data) written in MATLAB (MathWorks, Natick, MA, USA). Graph plotting and data analysis were performed with GraphPad Prism and MATLAB software. Statistical analysis was performed using two-tailed Student's *t* test. Standard *p*-value threshold of <0.05 was used to indicate statistical significance. *p* values were shown on the figures as asterisks: *, $p < 0.05$; **, $p < 0.01$; ***, $p < 0.001$; ****, $p < 0.0001$.